DOI: 10.1002/chem.201203644

Group IV Organometallic Compounds Based on Dianionic "Pincer" Ligands: Synthesis, Characterization, and Catalytic Activity in Intramolecular Hydroamination Reactions

Lapo Luconi,[a] Andrea Rossin,[a] Alessandro Motta,[b] Giulia Tuci,[a] and Giuliano Giambastiani*[a]

In memory of Stefano Midollini

Abstract: Neutral Zr^{IV} and Hf^{IV} diamido complexes stabilized by unsymmetrical dianionic N,C,N′ pincer ligands have been prepared through the simplest and convenient direct metal-induced C_{aryl}–H bond activation. Simple ligand modification has contributed to highlight the non-innocent role played by the donor atom set in the control of the cyclometallation kinetics. The as-prepared bis-amido catalysts were found to be good candidates for the intramolecular hydroamination/cyclization of primary aminoalkenes. The ability of these compounds to promote such a catalytic transformation efficiently (by providing, in some cases, fast and complete substrate conversion at room temperature) constitutes a remarkable step forward toward catalytic systems that can operate at relatively low catalyst loading and under milder reaction conditions. Kinetic studies and substrate-scope investigations, in conjunction with preliminary DFT calculations on the real systems, were used to elucidate the effects of the substrate substitution on the catalyst performance and to support the most reliable mechanistic path operative in the hydroamination reaction.

Keywords: C–H activation · hafnium · hydroamination · pincer complexes · zirconium · σ-bond metathesis

Introduction

The control of single-site catalysts efficiency by tailoring ligand frameworks is an ultimate goal and a challenging matter for many inorganic and organometallic chemists. Indeed, the ability to vary the steric and electronic properties of a given ligand provides a powerful tool to tune reactivity, stability, catalytic performance, and other important features of the metal center. On this basis, aryl-based (*E*,C,*E*)-pincer transition-metal complexes with anionic tridentate ligands have been widely applied in organic synthesis, organometallic catalysis, and other related areas.[1] Their basic structure consists of a central σ-bonded aryl donor group (C) capable of forming robust M–C bonds with a given metal center, enforced by the synergic effect of both the coordination of peripheral donor groups (*E*) and the chelating rigid structure of the (*E*,C,*E*) ligand framework. Such a combination typically results in systems that feature a unique balance of stability versus reactivity. Synthetically, the simplest method for the construction of these complexes is the direct metal-induced C_{aryl}–H bond activation, which can be fulfilled by choosing the appropriate neutral or anionic functional donor groups (*E*) at the two sidearms of the pincer moiety. Transition-metal organometallic compounds featured by either monoanionic or trianionic (i.e., N,C^-,N; N^-,C^-,N^-) pincer-type motifs have been extensively investigated in recent years, thus revealing remarkable and to some extent unique catalytic properties in selected fields of organometallic catalysis.[1] Most importantly, the easy tuning of the hardness of the N donor has led to the isolation of a large variety of complexes with metal centers that span from alkaline-earth metals to those of the Group 12 late transition series (Zn→Hg).[1,2] Although a relatively large number of NCN-pincer-type complexes containing metal centers of Groups 8–10 have been reported to date, much less work has been done for the synthesis and characterization of the early-based counterparts.[1a,3] In addition, most of the NCN-pincer complexes are symmetrical with two identical N donors[1,4] (because of the easier synthetic protocols that can be adopted for their preparation), whereas unsymmetrical NCN′-systems are rather uncommon and limited (to the best of our knowledge) to an unique example based on palladium derivatives.[1i,5–7]

[a] Dr. L. Luconi, Dr. A. Rossin, Dr. G. Tuci, Dr. G. Giambastiani
Institute of Chemistry of Organometallic Compounds
ICCOM-CNR and Consorzio INSTM, Via Madonna del Piano
10–50019 Sesto F.no Florence (Italy)
Fax: (+39) 055-5225203
E-mail: giuliano.giambastiani@iccom.cnr.it

[b] Dr. A. Motta
Dipartimento di Scienze Chimiche
University of Catania and INSTM Udr of Catania
V.le A. Doria, 6–95125 Catania (Italy)

Supporting information for this article is available on the WWW under http://dx.doi.org/10.1002/chem.201203644.

© 2013 Wiley-VCH Verlag GmbH & Co. KGaA, Weinheim
WILEY ONLINE LIBRARY
These are not the final page numbers!

Research in our group has a long-lasting tradition in the design and synthesis of ligand systems that combine hard donating atoms (N and C) with additional coordinating donor groups.[8] Their combination with a large variety of transition-metal and rare-earth metal centers has provided a number of catalyst precursors for efficient olefin upgrading[8,9] (oligomerization, polymerization, and copolymerization) and aminoalkene hydroamination.[10] If developing catalysts that can operate efficiently under increasing temperature processes in solution represents a key issue in catalysis, thus preparing robust and thermally stable systems is a challenging and highly desirable goal. By starting from our recent interest in Group IV pyridylamido catalysts,[9–11] a rethink of their molecular framework, while maintaining the same donor atom set, has resulted in a step forward toward more thermally stable and catalytically active systems (Figure 1).

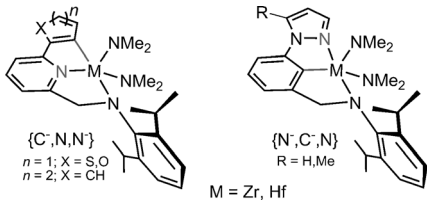

Figure 1. Left: State of the art Group IV pyridylamido complexes.[8–10] Right: Group IV NCN′-pincer complexes from this study.

Herein, we describe a new set of pincer ligands and their use for preparing nonsymmetrical Group IV complexes bearing dianionic N,C$^-$,N$^-$-pincer fragments. The donor-atom set includes a pyridinic nitrogen atom from the poor π-acceptor pyrazole ring (as a harder donor site relative to classical pyridine units),[12] in conjunction with other two hard coordination sites form the aryl central unit (C$^-$) and the amido pendant arm (N$^-$), respectively. With $[Zr(NMe_2)_4]$ and $[Hf(NMe_2)_4]$ as metal precursors under mild reaction conditions, monosubstituted $[M^{IV}(\kappa\text{-}N\text{-L})(NMe_2)_3]$ (L = ligand) complexes bearing a "dangling" intact C–H aryl bond are isolated and completely characterized by using a simple transamination reaction. The prolonged heating of these complexes in solution leads to the formation of thermally stable $[M^{IV}(\kappa^3\text{-}N,C,N\text{-L})(NMe_2)_2]$ pincer species through a successive metal–ligand σ-bond metathesis (Figure 1, right). To the best of our knowledge, this example is the first of thermally stable, unsymmetrical dianionic N,C,N′ Group IV metal complexes reported to date.[13] Simple modifications of the ligand framework result in a remarkable increase of the cyclometallation kinetics, thus highlighting the non-innocent role played by the pyrazole moiety. The as-synthesized neutral pincer-diamido complexes were good candidates for the intramolecular hydroamination/cyclization of primary aminoalkenes.[10,14,15] In particular, the $[Zr^{IV}(\kappa^3\text{-}N,C,N\text{-L})(NMe_2)_2]$ derivative showed a remarkable hydroamination activity with selected aminoalkenes, thus providing fast and complete substrate conversion at room temperature. Kinetic measurements and substrate-scope investigations, in conjunction with DFT calculations on the whole systems, were used to elucidate the effects of the substrate substitution on the catalyst performance and to support the most reliable mechanistic path operative for these systems.

Results and Discussions

Synthesis of the N,C,N-pincer ligands H_2L 4 and H_2L^{Me} 12: Scheme 1 illustrates the stepwise procedure developed to prepare the desired pincer ligands in fairly good yields. Because this synthesis work was not technically trivial (at least for the methylated ligand H_2L^{Me}) and may be useful for the design of other related molecular architectures, a description of the most relevant reaction steps is given.

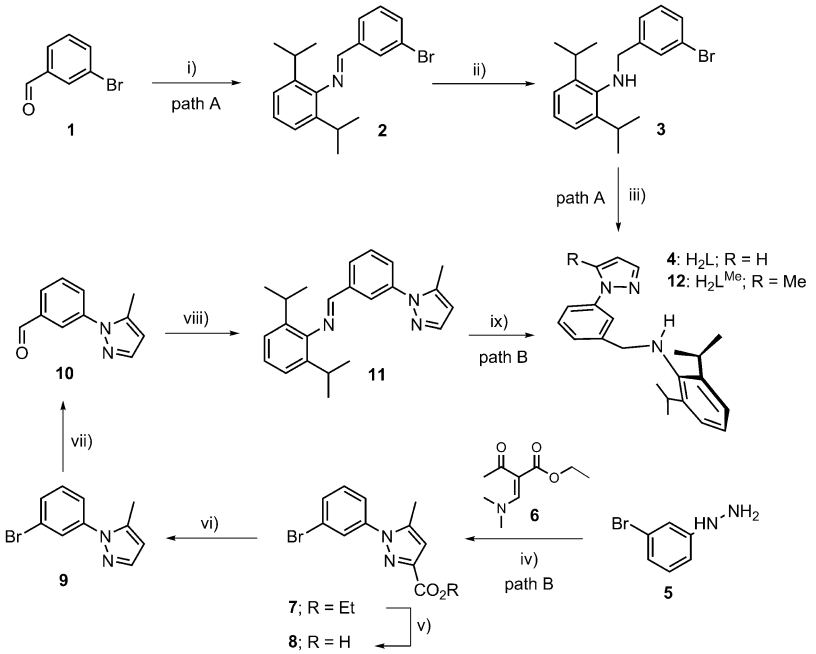

Scheme 1. Synthesis of the pincer ligands **4** and **12**. Reagents and conditions: Path A with H_2L: i) 2,6-diisopropyl aniline, *p*-TSA cat., toluene, reflux; ii) $NaBH_3CN$, AcOH, THF/MeOH; iii) pyrazole; CuI, NMP, microwave irradation, 210 °C, 5 h, 250 W. Path B with H_2L^{Me}: iv) **6**, EtOH; reflux, 2 h; v) LiOH, EtOH/H_2O, 80 °C, 16 h; vi) neat **8**, 215 °C, 60 h; vii) HCOONa, DMF, $[Pd(PPh_3)_2Cl_2]$ cat., CO, 110 °C, 1 h; viii) see (i); ix) see (ii). NMP = *N*-methylpyrrolidone, *p*-TSA = *para*-toluenesulfonic acid.

© 2013 Wiley-VCH Verlag GmbH & Co. KGaA, Weinheim

These are not the final page numbers!

Two different strategies were developed to prepare ligands **4** and **12** (Scheme 1). Path A was followed to prepare **4** in a three-step synthesis, whereas the introduction of a methyl group on the pyrazolyl moiety of **12** required a slightly more complex approach (see path B in Scheme 1). According to path A in Scheme 1, 3-bromobenzaldehyde (**1**) was straightforwardly converted into the imine derivative **2** under classical condensation conditions in the presence of a catalytic amount of PTSA by using a Dean–Stark apparatus.[16]

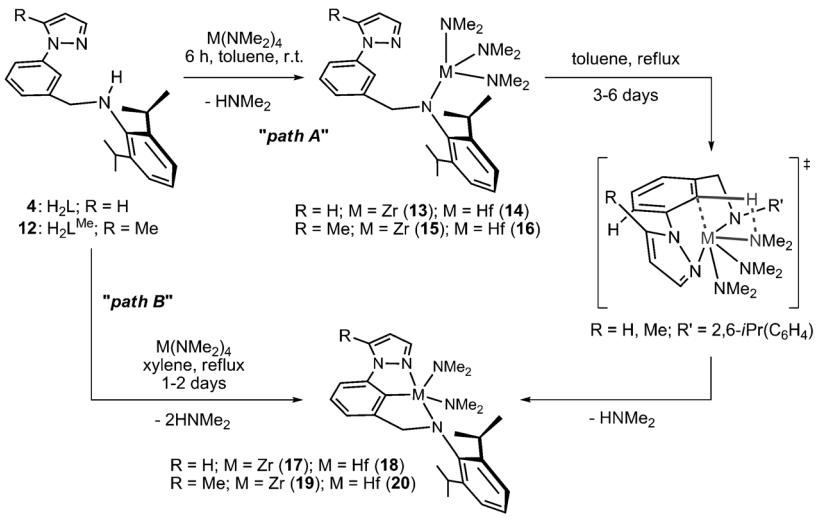

Scheme 2. Synthesis of the $[M^{IV}(\kappa\text{-}N\text{-}HL^{R})(NMe_2)_3]$ (**13**–**16**) and $[M^{IV}(\kappa^3\text{-}N,C,N\text{-}L^{R})(NMe_2)_2]$ (**17**–**20**; M = Zr, Hf) complexes.

The subsequent imine reduction by treatment with $NaCNBH_3$/AcOH[17] resulted in the formation of the corresponding secondary aniline derivative **3**. A Cu-catalyzed Ullmann coupling between **3** and pyrazole under microwave irradiation/heating[18,19] gave the expected H_2L pincer ligand **4** after chromatographic purification in the form of off-white crystals in 68% yield of the isolated product over three synthetic steps (see the Experimental Section).

Commercially available 3-bromophenylhydrazine (**5**) was used as the starting material to synthesize the methylated pyrazolyl ligand H_2L^{Me} **12**. The reaction of ethyl 2-[(dimethylamino)methylene] methyl-3-oxobutanoate (**6**) with **5** gave the 3,5-disubstituted pyrazolyl **7** in fairly good yield.[20] Successive ethyl ester hydrolysis[21] followed by thermal decarboxylation afforded the desired 1-(3-bromophenyl)-5-methyl-1*H*-pyrazole (**9**) intermediate. Pd-catalyzed formylation[22] followed by reductive amination[16,17] gave the desired pincer ligand **12** in 55% yield of the isolated product over six synthetic steps (see the Experimental Section).

Synthesis and characterization of Group IV metal/amido complexes from the H_2L and H_2L^{Me} ligands: The reaction of both ligands **4** and **12** with either $[Zr(NMe_2)_4]$ or $[Hf(NMe_2)_4]$ in toluene was followed by ^1H NMR spectroscopic analysis until completeness. Ligand consumption took place at room temperature, with the progressive disappearance of distinctive signals attributed to the uncoordinated system. After 6 hours of stirring at room temperature, unique tris-amido species were generated, irrespective of the ligand or metal precursor used (Scheme 2, path A). All the ^1H and $^{13}C(^1H)$ NMR spectra show similar patterns, with large superimposable spectral regions and no traces of low-field quaternary carbon atoms ascribable to the presence of cyclometallated forms (see Figures S19–S26 in the Supporting Information).[9,11] Although the occurrence of a transamination reaction was evidenced by the disappearance of the typical ligand broad singlet at the aniline moiety, no unequivocal proof of the effective coordination of the pyrazole moiety to the metal center could be found.

X-ray diffraction analyses of **13** and **14** have contributed to clarify the metal coordination sphere of the tris-amido complexes. A perspective view of both complexes are given in Figures 2 and 3, whereas selected bond lengths and angles

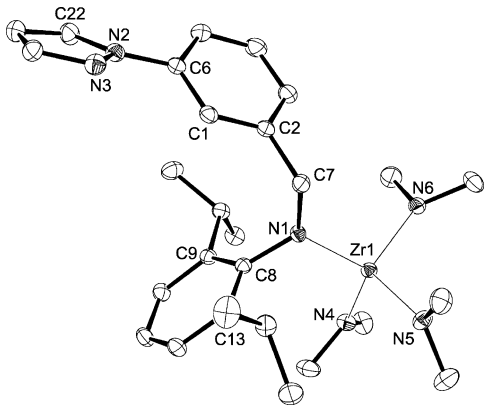

Figure 2. Crystal structure of $[Zr^{IV}(\kappa\text{-}N\text{-}HL)(NMe_2)_3]$ (**13**). Thermal ellipsoids are drawn at the 40% probability level. Hydrogen atoms are omitted for clarity.

are listed in Table 2. In both systems, the metal coordination environment appears to be tetrahedral, with three dimethylamido groups and one amido moiety from the monoanionic N,C,N$^-$ ligand. The pyrazolyl moieties are tilted with respect to the central aryl unit (torsion angle θ [°] of C1-C6-N2-N3: **13**: 30.9(2), **14**: −30.4(7)) and point away from the metal coordination sphere. Such metal environments are likely due to the contribution of steric and electronic factors, the latter being mainly attributed to the decreased basicity of the pyrazole nitrogen atom[23] if compared to a classical pyridine unit. For both compounds, two almost identical molecules

 © 2013 Wiley-VCH Verlag GmbH & Co. KGaA, Weinheim

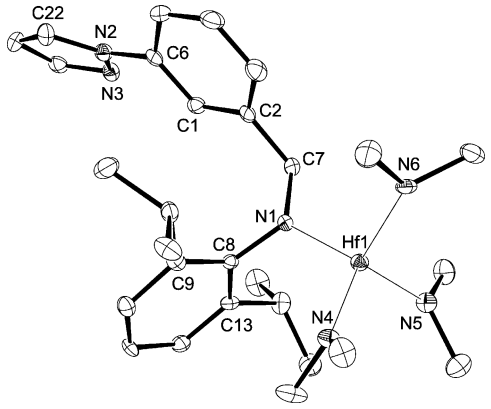

Figure 3. Crystal structure of $[Hf^{IV}(\kappa\text{-}N\text{-}HL)(NMe_2)_3]$ (**14**). Thermal ellipsoids are drawn at the 40% probability level. Hydrogen atoms are omitted for clarity.

are present in the asymmetric unit; they are related to each other through a C_2 pseudosymmetry axis along the *b* direction. Consequently, the same chemical species is "seen" as two structurally different molecules.[24] Table 1 reports all the main crystal and structural-refinement data.

Prolonged heating of all the tris-amido species **13**–**16** in toluene at reflux provided bis-amido derivatives **17**–**20** as a result of an intramolecular orthometallation/pyrazolyl coordination to the metal center (Scheme 2, path A). The as-synthesized pentacoordinate complexes were isolated as air- and moisture-sensitive microcrystals and were completely characterized by spectroscopic data (see the Supporting Information) and X-ray diffraction studies. The ^1H and $^{13}C\{^1H\}$ NMR patterns indicate that all the complexes possess C_s symmetry in solution. The most relevant ^1H and $^{13}C\{^1H\}$ NMR spectroscopic resonances related to the κ^3-coordinated ligand framework fall at lower field relative to those observed in the tris-amido precursors **13**–**16**. Notably, the M–C^{Ar} bonds generated upon intramolecular cyclometallation are unambiguously evidenced by a remarkable resonance shift to lower fields of the aromatic carbon atoms directly bound to the metal center ($\delta = 174.0$, 181.8, 175.5, and 183.1 ppm for **17**–**20**, respectively). All the complexes are highly soluble in aromatic hydrocarbon compounds, whereas they are only sparingly soluble in *n*-pentane. Accordingly, suitable crystals for X-ray analyses were isolated from concentrated and cold *n*-pentane/toluene solutions. ORTEP representations of the crystal structures of **17**–**20** are given in Figures 4–7. Table 1 lists all the main crystal and structural-refinement data, whereas selected bond lengths and angles are summarized in Table 2.

Table 1. Crystal data and structure refinement for complexes **13**, **14**, and **17**–**20**.

	13	**14**	**17**	**18**·0.5 C_5H_{12}	**19**	**20**
CCDC number	897882	897880	897878	897881	897879	897883
formula	$C_{28}H_{44}N_6Zr$	$C_{28}H_{44}HfN_6$	$C_{26}H_{37}N_5Zr$	$C_{26}H_{37}HfN_5 \cdot 0.5\,C_5H_{12}$	$C_{27}H_{39}N_5Zr$	$C_{27}H_{39}HfN_5$
M_r	555.91	643.18	510.83	634.17	524.85	612.12
T [K]	120(2)	120(2)	150(2)	120(2)	150(2)	120(2)
μ [nm]	0.71069	0.71069	0.71079	0.71069	0.71069	0.71069
crystal system	triclinic	triclinic	triclinic	triclinic	monoclinic	monoclinic
space group	$P\bar{1}$	$P\bar{1}$	$P\bar{1}$	$P\bar{1}$	$P2_1/n$	$P2_1/n$
a [Å]	9.292(3)	9.313(4)	8.722(4)	11.202(5)	12.512(2)	12.468(2)
b [Å]	16.458(6)	16.442(6)	9.077(5)	16.516(8)	15.094(2)	14.965(2)
c [Å]	19.607(6)	19.637(9)	18.248(8)	17.669(9)	14.823(3)	14.873(3)
α [°]	77.704(3)	77.568(3)	96.749(4)	64.542(5)	90	90
β [°]	82.857(3)	82.947(4)	101.692(4)	83.354(4)	99.818(18)	99.793(17)
γ [°]	86.290(3)	86.442(3)	109.978(4)	83.026(4)	90	90
V [Å^3]	2904.7(16)	2912.2(19)	1301.9(11)	2922.4(18)	2758.4(13)	2734.6(8)
Z, ρ_{calcd} [g m^{-3}]	4, 1.271	4, 1.467	2, 1.303	4, 1.441	4, 1.264	4, 1.487
μ [mm^{-1}]	0.404	3.608	0.444	3.593	0.421	3.837
F(000)	1176	1304	536	1284	1104	1232
crystal size [mm]	0.040.040.06	0.010.010.02	0.010.010.02	0.01 0.0150.03	0.050.050.07	0.030.030.05
range for data collection	4.10/32.58	4.19/29.47	4.16/29.37	4.14/32.95	4.17/29.25	4.18/29.35
limiting indices	$13 \le h \le 13$ $24 \le k \le 24$ $29 \le l \le 29$	$11 \le h \le 12$ $22 \le k \le 21$ $24 \le l \le 27$	$11 \le h \le 11$ $12 \le k \le 12$ $24 \le l \le 24$	$15 \le h \le 16$ $24 \le k \le 24$ $26 \le l \le 26$	$15 \le h \le 15$ $18 \le k \le 20$ $19 \le l \le 19$	$16 \le h \le 16$ $19 \le k \le 19$ $18 \le l \le 19$
reflections collected/unique	55455/19200	23903/13346	28661/6277	44830/19269	47863/6845	35576/6694
GOF on F^2	0.962	1.000	1.041	1.074	1.041	1.048
data/restraints/parameters	19200/0/651	13346/0/651	6277/0/297	19269/0/640	6845/0/307	6694/0/307
final R indices [$I > 2(I)$]	$R1 = 0.0371$, $wR2 = 0.0833$	$R1 = 0.0439$, $wR2 = 0.0729$	$R1 = 0.0383$, $wR2 = 0.0839$	$R1 = 0.0372$, $wR2 = 0.0802$	$R1 = 0.0664$, $wR2 = 0.1464$	$R1 = 0.0335$, $wR2 = 0.0686$
R indices (all data)	$R1 = 0.0587$, $wR2 = 0.0951$	$R1 = 0.0695$, $wR2 = 0.0831$	$R1 = 0.0513$, $wR2 = 0.0905$	$R1 = 0.0543$, $wR2 = 0.0924$	$R1 = 0.1054$, $wR2 = 0.1691$	$R1 = 0.0478$, $wR2 = 0.0751$
largest diff. peak and hole [e Å^{-3}]	0.572 and 0.784	1.483 and 2.036	0.702 and 0.421	2.905 and 2.140	1.361 and 1.023	1.435 and 1.339

© 2013 Wiley-VCH Verlag GmbH & Co. KGaA, Weinheim

These are not the final page numbers!

Table 2. Selected bond lengths [Å] and angles [°] for complexes **13**, **14**, and **17**–**20**.

	13[a]	**14**[a]	**17**	**18**·0.5 C_5H_{12}[a]	**19**	**20**
M–N1	2.0845(16)	2.067(4)	2.1055(19)	2.108(3)	2.127(3)	2.103(3)
M–N3	–	–	2.365(2)	2.328(3)	2.308(4)	2.292(4)
M–N4	2.0353(16)	2.020(4)	2.045(2)	2.032(3)	2.034(4)	2.013(4)
M–N5	2.0452(15)	2.031(4)	2.058(2)	2.040(3)	2.025(5)	2.024(4)
M–N6	2.0229(16)	2.015(4)	–	–	–	–
M–C1	–	–	2.238(2)	2.229(3)	2.247(4)	2.220(4)
N2–N3	1.352(2)	1.359(5)	1.367(3)	1.375(4)	1.360(6)	1.358(5)
N1–C7	1.470(2)	1.482(6)	1.470(3)	1.480(4)	1.461(5)	1.468(5)
N1-M-N3	–	–	139.75(7)	141.77(10)	140.11(14)	141.35(13)
N1-M-N4	114.83(6)	113.80(16)	112.12(7)	111.03(12)	111.92(16)	110.94(15)
N1-M-N5	109.78(6)	110.08(16)	107.45(8)	108.38(11)	108.08(18)	107.96(16)
N1-M-N6	108.30(6)	108.58(17)	–	–	–	–
N1-M-C1	–	–	72.86(8)	73.76(12)	72.98(13)	73.84(13)
N3-M-C1	–	–	68.22(8)	68.95(11)	67.71(15)	68.24(14)
N4-M-C1	–	–	130.11(8)	128.61(12)	127.34(16)	128.38(15)
N5-M-C1	–	–	111.93(9)	115.51(13)	114.8(3)	114.9(2)
N4-M-N5	105.85(6)	106.29(18)	112.99(8)	111.01(13)	112.8(3)	111.9(2)
C1-C2-C7-N1	103.21(18)	−103.5(5)	3.2(3)	9.6(4)	−1.4(5)	0.9(5)
C1-C6-N2-N3	30.9(2)	−30.4(7)	−1.3(3)	−3.9(4)	4.5(6)	−4.2(5)
C7-N1-C8-C9	106.63(17)	−106.3(5)	90.5(2)	−80.7(4)	89.4(4)	89.8(4)
C29-C34-N8-N9[a]	−23.0(2)	−22.4(8)	–	–	–	–
C27-C32-N7-N8[a]	–	–	–	−0.07(6)	–	–

[a] Selected dihedral angles of the second molecule in the asymmetric unit. M = Zr^{IV} or Hf^{IV}

For all the isolated species, the coordination environment at the metal center consists of two nitrogen atoms and one carbon atom from the dianionic tridentate N,C^-,N^- ligand (κ^3-coordination) and two dimethylamido fragments. All the complexes show a distorted square-pyramidal coordination geometry, with the ligand donor atoms and one dimethylamido group lying equatorially and a residual $-NMe_2$ fragment that occupies the axial position.[26]

The κ^3-coordinated fragments are almost planar, with the pyrazolyl moieties slightly tilted away from the phenyl central core (θ(C1-C6-N2-

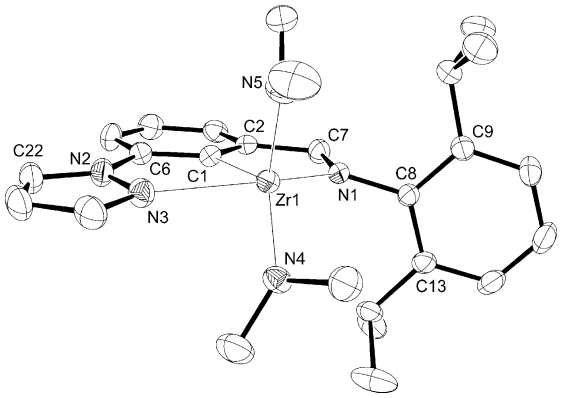

Figure 4. Crystal structure of [Zr^{IV}(κ^3-*N*,*C*,*N*-L)(NMe_2)$_2$] (**17**). Thermal ellipsoids are drawn at the 40% probability level. Hydrogen atoms are omitted for clarity.

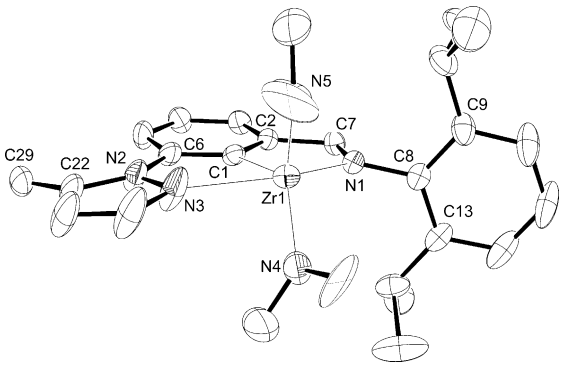

Figure 6. Crystal structure of [Zr^{IV}(κ^3-*N*,*C*,*N*-L^{Me})(NMe_2)$_2$] (**19**). Thermal ellipsoids are drawn at the 40% probability level. Hydrogen atoms are omitted for clarity.

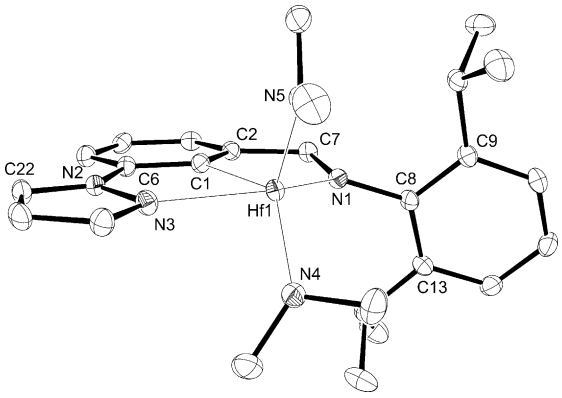

Figure 5. Crystal structure of [Hf^{IV}(κ^3-*N*,*C*,*N*-L)(NMe_2)$_2$] (**18**). Thermal ellipsoids are drawn at the 40% probability level. Hydrogen atoms and molecules of the solvent of crystallization (pentane) are omitted for clarity.[25]

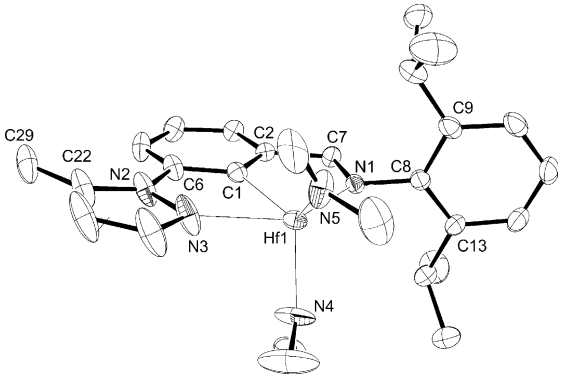

Figure 7. Crystal structure of [Hf^{IV}(κ^3-*N*,*C*,*N*-L^{Me})(NMe_2)$_2$] (**20**). Thermal ellipsoids are drawn at the 40% probability level. Hydrogen atoms are omitted for clarity.

© 2013 Wiley-VCH Verlag GmbH & Co. KGaA, Weinheim

N3) = −1.3(3), −3.9(4), 4.5(6), and −4.2(5)° for **17–20**, respectively). For all the complexes, the M−N1, M−N3, and M−C1 distances fall in a similar range to those measured for related structures[27–29] (i.e., M−N1 = 2.1055(19), 2.108(3), 2.127(3), and 2.103(3) Å; M−N3 = 2.365(2), 2.328(3), 2.308(4), and 2.292(4) Å; and M−C1 = 2.238(2), 2.229(3), 2.247(4), and 2.220(4) Å for **17–20**, respectively).

The as-synthesized pentacoordinated species showed a remarkable thermal stability, with no apparent decomposition even after six days under reflux in toluene. It is worth noting that precursors bearing a methylpyrazole fragment (i.e., **15** and **16**) showed faster orthometallation kinetics, with the complete generation of the cyclometallated species up to twice as fast as the counterparts containing plain pyrazole moieties (Table 3, entry 1 vs. entries 5 and 3 vs. entry 7). The reaction course was periodically monitored by collecting samples from the mixture at different times and following the consumption of the precursor(s) by ^{1}H NMR spectroscopic analysis (inside a NMR capillary tube filled with [D_8]toluene) until completeness.

Table 3. Reaction times and yield of the isolated products for **17–20**.

Entry	Precursor(s)	Product	T [°C]	t [h][a]	Yield [%]
1[b]	**13**	**17**	110	145	85[e]
2[c]	**4** + [Zr(NMe$_2$)$_4$][d]	**17**	138	70	87
3[b]	**14**	**18**	110	135	77[f]
4[c]	**4** + [Zr(NMe$_2$)$_4$][d]	**18**	138	70	79
5[b]	**15**	**19**	110	70	86[g]
6[c]	**12** + [Zr(NMe$_2$)$_4$][d]	**19**	138	30	86
7[b]	**16**	**20**	110	65	83[h]
8[c]	**12** + [Hf(NMe$_2$)$_4$][d]	**20**	138	24	85

[a] The reaction course was followed by collecting samples from the reaction mixtures at different reaction times till completeness and by analyzing the crude products by ^{1}H NMR spectroscopy (inside NMR capillary tubes filled with [D_8]toluene). [b] Toluene was the solvent. [c] Xylene was the solvent. [d] Ratio of ligand/metal precursor = 1:1.05. [e] Yield of the isolated product was 82% over two reaction steps. [f] Yield of the isolated product was 72% over two reaction steps. [g] Yield of the isolated product was 82% over two reaction steps. [h] Yield of the isolated product was 76% over two reaction steps.

Compounds **17–20** were prepared in a single step from a ligand/metal precursor mixture with xylene as the solvent to optimize the reaction conditions and chemical yields (Scheme 2, path B). The yields of the isolated products were improved for all runs (Table 3). In addition, by increasing the reaction temperature of about 20 °C (from toluene at reflux to xylene at reflux) resulted in a remarkable speeding up of the orthometallation kinetics (Table 3, even vs. odd entries). Compounds **19** and **20** were obtained as pure microcrystalline solids after 24–30 hours of heating to reflux, whereas the non-methylated counterparts (i.e., **17** and **20**) required reaction times that were over threefold longer to reach completeness. Such a result is reasonably due to the simultaneous occurrence of stereoelectronic factors.

In particular, the coordination of the free pyrazole nitrogen atom of the heteroaromatic moiety to the metal center is assumed to be crucial in assisting the subsequent cyclometallation step. Theoretical simulations carried out on the real systems **13** and **15** have shown a significant increase of the dihedral angle θ(C1-C6-N2-N3) for the latter optimized conformer (Figure 8).

The main source of the pyrazolylphenyl deviation from coplanarity is the presence of H−H eclipsing interactions between the proton atoms of the methyl group at the pyrazolyl fragment (i.e., **15** and **16**) and the hydrogen atom of the phenyl central unit (see Scheme 2 for the supposed transition state (TS)).

Although no evidence of *N*-pyrazolyl coordination to the metal center before the cyclometallation step can be unambiguously provided for precursors **13** and **14**, it seems reasonable that only assistance from the pyrazolyl unit can be invoked to justify the increased cyclometallation kinetics for the methylated intermediates **15** and **16**.[30]

Relative to other Group IV N,C,N systems, our synthetic approach maintains three residual amido groups at the metal center prior to the cyclometallation step (see intermediates **13–16** and the TS in Scheme 2). Such an aspect, in combination with the coordination ability of the pyrazolyl moiety, represents a fundamental prerequisite to succeed in the central aryl C−H bond activation at which other related synthetic approaches have failed.[3d]

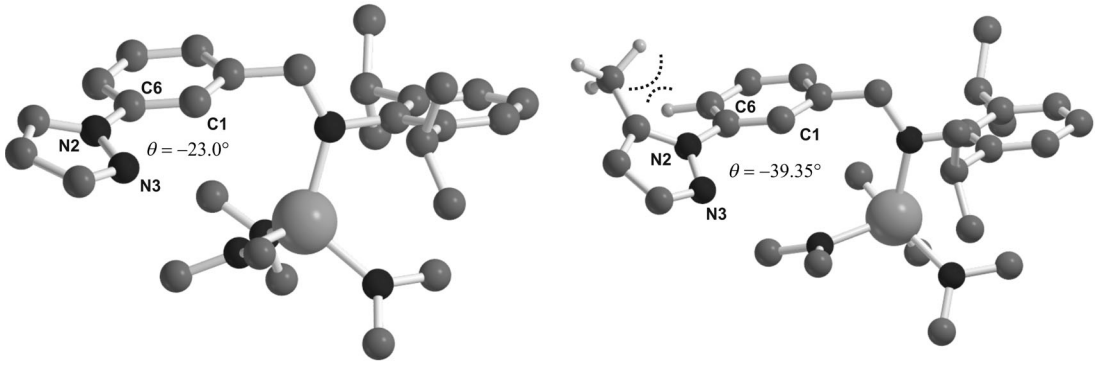

Figure 8. Gas-phase optimized structures (DFT//M06) of **13** (left) and **15** (right). Hydrogen atoms not relevant for the discussion have been omitted for clarity. Atom color code: gray, C; white, H; black, N; light gray, Zr. The optimized C1-C6-N2-N3 dihedral angles between the phenyl and pyrazole rings are also reported.

© 2013 Wiley-VCH Verlag GmbH & Co. KGaA, Weinheim

These are not the final page numbers!

Catalytic performance of novel amido complexes in the intramolecular hydroamination of aminoalkenes: All the isolated amido compounds were tested as catalysts for the intramolecular hydroamination/cyclization of primary and secondary amines tethered to monosubstituted alkenes (see Scheme 3 and Table 4).

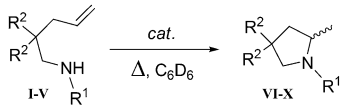

I R^2 = Ph R^1 = H
II R^2 = -$(CH_2)_5$- R^1 = H
III R^2 = CH_3 R^1 = H
IV R^2 = H R^1 = H
V R^2 = Ph R^1 = Me

Scheme 3. Intramolecular hydroamination of primary and secondary aminoalkenes.

Table 4. Intramolecular hydroamination of primary and secondary aminoalkenes catalyzed by neutral amido complexes **13**, **14**, and **17**–**20**.[a]

Entry	Catalyst	Substrate	Product	T [°C]	t [h]	Conver. [%][b]
1	**17**	**I**	**VI**	rt	3	96
2	**17**	**I**	**VI**	rt	5	>99
3	**17**	**I**	**VI**	50	1	98
4	**17**	**I**	**VI**	80	0.5	>99
5	**19**	**I**	**VI**	rt	5	>99
6	**19**	**I**	**VI**	50	1	96
7	**17**	**II**	**VII**	rt	48	40
8	**17**	**II**	**VII**	80	36	87
9[c]	**17**	**II**	**VII**	110	1.5	95
10	**17**	**III**	**VIII**	rt	48	9
11	**17**	**III**	**VIII**	80	36	45
12[c]	**17**	**III**	**VIII**	110	4	78
13[c]	**17**	**IV**	**IX**	110	10	31
14	**17**	**V**	**X**	80	96	–[d]
15	**13**	**I**	**VI**	rt	3	12
16	**13**	**I**	**VI**	80	1	6
17	**18**	**I**	**VI**	rt	3	15
18	**18**	**I**	**VI**	50	1	91
19	**18**	**I**	**VI**	80	0.75	>99
20	**20**	**I**	**VI**	rt	3	17
21	**20**	**I**	**VI**	50	1	87
22	**18**	**II**	**VII**	80	36	67
23	**18**	**III**	**VIII**	80	36	38
24[c]	**18**	**III**	**VIII**	110	6	66
25[c]	**18**	**IV**	**IX**	110	10	14
26	**18**	**V**	**X**	80	96	–[d]
27	**14**	**I**	**VI**	rt	3	<1
28	**14**	**I**	**VI**	80	1	2

[a] Reaction conditions: substrate = 0.63 mmol, catalyst = 5 mol%, solvent = benzene (2 mL). [b] Determined by ^{1}H NMR spectroscopy in situ with ferrocene as an internal standard. [c] Toluene (2 mL) was the solvent. [d] No appreciable amount of cyclization product was observed.

The catalytic tests were conducted in a glovebox in an inert atmosphere by using a two-necked round flask equipped with a magnetic stirring bar and a septum for the progressive substrate addition through a syringe. Benzene (unless otherwise stated) was used as the reaction solvent and the catalyst content was fixed to 5 mol% for each run. Finally, the reaction temperature was systematically varied from room temperature (22°C) to the solvent at reflux. Neutral systems **17**–**20** were active catalysts for the intramolecular hydroamination reaction of model primary aminoalkenes that provided, for selected issues, relatively fast and complete substrate conversions already at room temperature (Table 4, entries 2 and 5).

Notably, a dramatic Thorpe–Ingold effect on the kinetics of the intramolecular hydroamination reaction is apparent (Table 4, entries 1 vs. 7 vs. 10). In particular, the diphenyl-substituted precursor **I** appears as the most suitable substrate that can convert into the corresponding cyclization product **VI** quantitatively within 5 hours under mild conditions (Table 4, entries 2 and 9). This result is certainly remarkable because only a few examples based on Group IV amido complexes reported refer to the complete cyclization of **I** under these mild reaction conditions (i.e., reaction temperature and catalyst loading).[15k,l,x,31]

With catalyst **17**, only geminally substituted substrates (**I**–**III**) undergo intramolecular hydroamination at room temperature with appreciable conversions (Table 4, entries 1, 7, and 10). On the contrary, prolonged heating in conjunction with higher reaction temperatures (toluene at reflux was used instead of benzene for selected issues) are required to give appreciable cyclization yield in the case of the unsubstituted substrate **IV** (Table 4, entries 13 and 25).

Although ligand modifications (**17** vs. **19** and **18** vs. **20**) did not show any appreciable difference in the activity of the catalyst (Table 4, entries 1 and 3 vs. 5 and 6; entries 17 and 18 vs. 20 and 21), experiments focused on comparing the Zr^{IV} and Hf^{IV} analogues (i.e., **17** vs. **18**) highlighted the higher catalytic performance of the former. Indeed, a conversion of **I** that was over sixfold higher was obtained with **17** instead of **18** (Table 4, entry 1 vs. 17). Notably, an increase of the reaction temperature translates into a significant decrease of the activity gap between the catalysts (Table 4, entries 2 and 4 vs. entries 17 and 19). Accordingly, **17** and **18** showed remarkable and almost similar activities for the complete conversion of **I** into **VI** when the reaction temperature was raised to the solvent reflux (Table 4, entry 4 vs. 19). Optimized reaction conditions are reported for the cyclization of the less sterically bulky aminoalkene precursors (**II**–**IV**). The highest the reaction temperature, the highest substrate cyclization, and the lowest the reaction time are given in Table 4 (entries 7–9, 10–12, and 17–19). It is worthy of note that an increase of the reaction temperature (from benzene to toluene at reflux) resulted in a dramatic decrease of the reaction time, together with significantly higher substrate conversions (Table 4, entries 8 vs. 9, 11 vs. 12, and 23 vs. 24). For all the investigated runs, the Zr^{IV} precursor compounds displayed higher catalytic performances relative to Hf^{IV} precursor compounds under similar reaction conditions. Aimed at highlighting the acceleration effects of the ligand in hydroamination reactions, the catalyst performance of **17** and **18** were compared with those of tris-amido precursors **13** and **14**. As it can be appreciated from Table 4, **13** and **14** present a significantly decreased catalytic activity relative to that of the related cyclo-

© 2013 Wiley-VCH Verlag GmbH & Co. KGaA, Weinheim

metallated bis-amido counterparts **17** and **18** (Table 4, entries 1 vs. 15 and 17 vs. 27). In addition, high reaction temperatures resulted in the lowest substrate conversions probably due to a more rapid metal/ligand displacement through a substrate-induced transamination reaction (Table 4, entries 4 vs. 16 and 19 vs. 28). Overall, these data highlight the outstanding substrate dependence on the catalytic performance of these novel pincer-type complexes. If it is generally accepted that decreasing the substrate steric demand translates into reduced cyclization efficiencies (**IV** ≪ **III** < **II** < **I**), such a trend is typically less marked than for the outcomes presented herein. Although **I** is rapidly and quantitatively transformed by **17** into the corresponding cyclization product **VI** at room temperature, either moderate conversions (for **II** and **III**) or no conversion at all (for **IV**) are given for the other substrates (see below) under similar conditions (Table 4, entry 1 vs. 7 vs. 10).

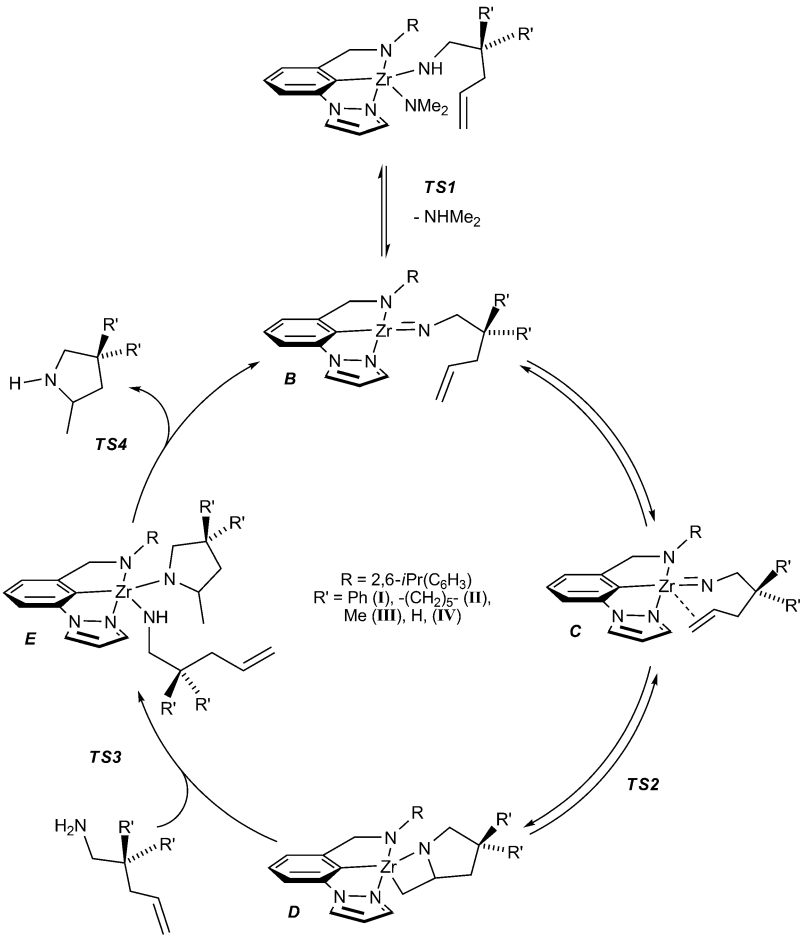

Scheme 4. [2+2]-Cycloaddition mechanism for the intramolecular hydroamination of primary aminoalkenes catalyzed by neutral bisamido Group IV metal complexes.

Finally, hydroamination of the secondary aminoalkene **V** does not take place with both **17** and **18**, even after prolonged heating (Table 4, entries 14 and 26), which is in agreement with most of the previous studies on neutral Group IV metal complexes in hydroamination reactions.[15,32] This observation also supports the hypothesis of imido species as intermediates in the catalytic cycle,[14,15] for which one of the most reliable representations is provided in Scheme 4.

In an attempt to shed light on the marked substrate dependence of catalyst **17** and to investigate possible and favorable substrate–complex interactions that can justify the observed outcomes, preliminary DFT calculations on the real systems **17**/**I** and **17**/**III** were carried out (Table 4, entries 1 vs. 10). In both cases, simulations were carried out on the whole systems that assume the formation of "imido species" (Scheme 4) as the most reliable mechanistic path (see also the Experimental section).[14,15,33] Accordingly, the relative internal energy profiles ($\Delta E = \Delta H$) for the two processes[34] have been calculated, and the energy values for the intermediates and transition states are outlined in Figure S40 (see the Supporting Information). In both cases, the energy profiles show similar trends, the formation of the imido species (TS1 and TS4) were the highest endothermic steps (TS1: $\Delta H = +33.4$ and $+35.2$ kcal mol^{-1} for **I** and **III**, respectively; TS4: $\Delta H = +37.3$ and $+38.1$ kcal mol^{-1} for **I** and **III**, respectively).[35]

The subsequent [2+2]-cycloaddition (Figure 9a) leads to the metalla-azacycle D intermediate (Scheme 4) through a fully reversible process for both aminoalkene precursors (3.3 kcal mol^{-1} and 0.7 kcal mol^{-1} for **I** and **III**, respectively). The protonolysis step (Figure 9b) takes place after the approach of a second substrate molecule, and it is considered to be an irreversible process, thus shifting the overall reaction to the products. Finally, an additional protonolysis reaction takes place, thus leading to the cyclization product with the regeneration of a novel imido species able to undergo further catalytic cycles (Figure 9c). It is worthy of note that all the transition states associated with protonolysis events (and potentially eligible as rate-limiting steps) are in line with the cyclization kinetics experimentally measured for precursor **I** and **III**, respectively ($\Delta(\Delta E^{\#}) = 0.8$ kcal mol^{-1} calculated for TS3 and TS4). Finally, negligible differences are observed in the optimized geometries of all the intermediates and transition states associated with both profiles. All these data taken together lead us to conclude that any pref-

© 2013 Wiley-VCH Verlag GmbH & Co. KGaA, Weinheim

These are not the final page numbers!

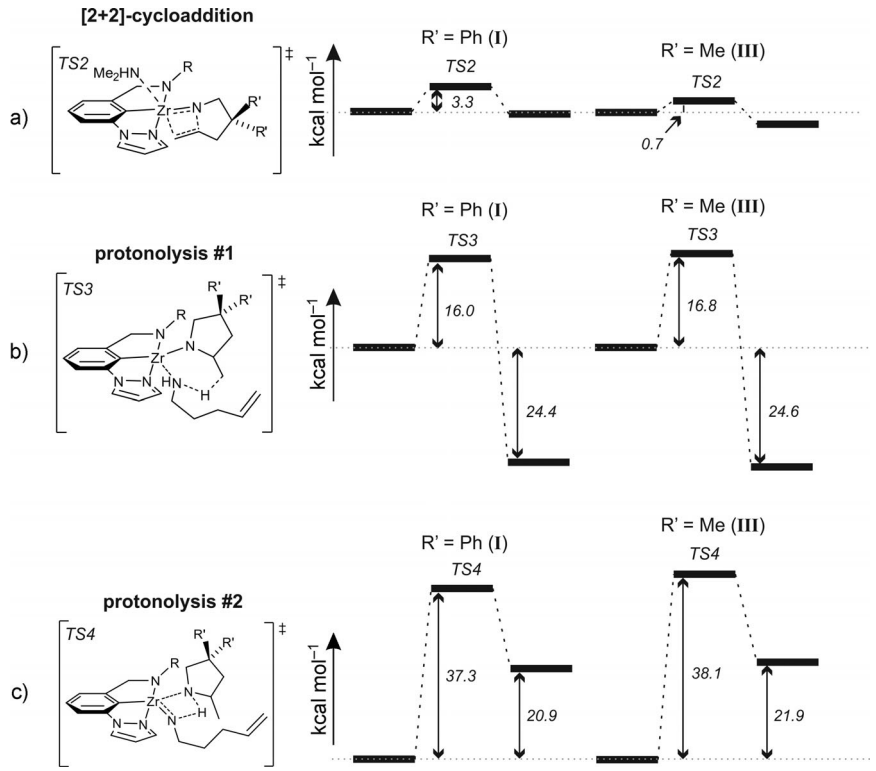

Figure 9. Calculated energetic profiles ($E=H$) for relevant transition states in the hydroamination/cyclization of **I** and **III** catalyzed by **17**. Imido mechanism (Scheme 4) is assumed as the most realistic for the catalytic systems employed in the present study. Labeling refers to Scheme 4, and see also Figure S40 in the Supporting Information for the complete energy profiles.[35]

erential substrate/complex interaction can be reasonably ruled out. It seems therefore apparent that the remarkable acceleration measured in the hydroamination of substrate **I** is exclusively ascribable to a *gem* effect originated by the dangling phenyl groups.[15o]

Kinetic investigations of **17** and **18** confirmed the first-order kinetics in substrate conversion, consistent with the protonolysis event as the rate-limiting step of the process.[15a] Figure 10 presents kinetic profiles measured at room temperature (only for **17**; Figure 10, left) and at 80 °C (**17** and **18**; Figure 10, right). A comparison of half-lives $t^1/_2$ of the catalyst is provided for both systems under optimized reaction conditions (80 °C; Table 4, entries 4 and 19). The measured $t^1/_2$ values were 4.76 and 21.5 minutes, respectively (Figure 10, right).[36]

In addition, Figure 11 shows the normalized Ln[substrate] versus time plots measured for three different concentrations of the most active system **17**, whereas the inset of the figure accounts for the linearity of the observed K_{obs} values versus catalyst concentration. All these data taken together are in accordance with first-order kinetics with respect to the catalyst and substrate concentration, as previously reported for other neutral zirconium systems.[15]

Conclusion

Overall, this study has provided a convenient way for the preparation of unsymmetrical dianionic N,C,N′ Group IV pincer complexes and has proved their successful application in the intramolecular hydroamination reaction of primary aminoalkenes. A proper choice of both ligand donor-atom set and substituents led to an easier aryl C–H bond activation (by intramolecular σ-bond metathesis), where other recent and related synthetic approaches failed.[3d] A non-innocent role of the *N*-coordinating pyrazolyl moiety was finally invoked to rationalize the cyclometallation kinetic gap measured in the presence of the H_2L and H_2L^{Me} ligands, respectively. To the best of our knowledge, this class of compound represents the first

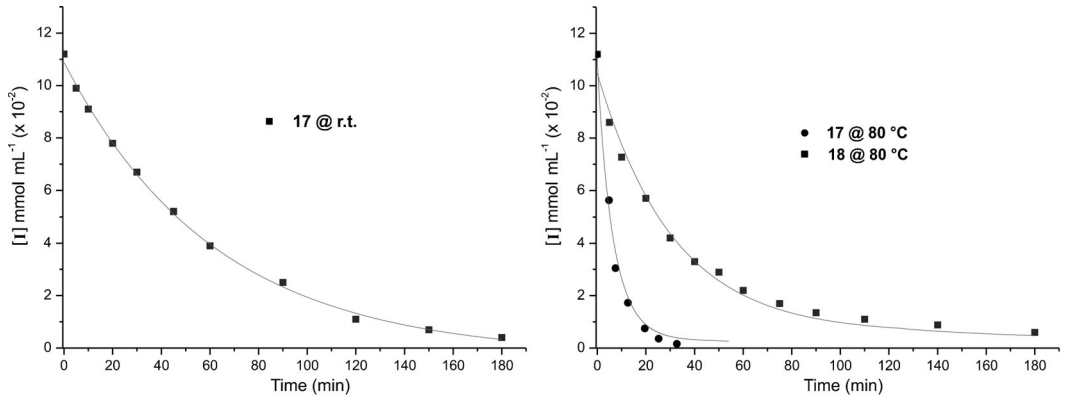

Figure 10. Plot of first-order substrate **I** conversion by using 5 mol % of **17** at room temperature (left) and 5 mol % of **17** and **18** at 80 °C (right). The catalyst half-lives have been determined for runs at 80 °C (right).

© 2013 Wiley-VCH Verlag GmbH & Co. KGaA, Weinheim

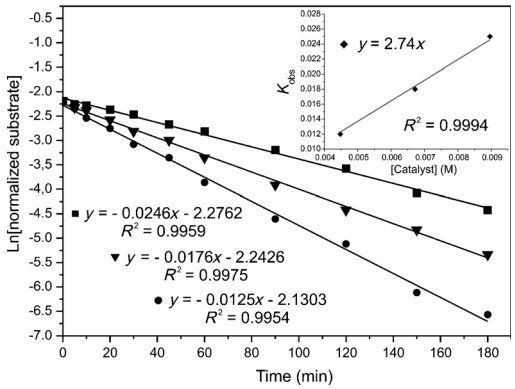

Figure 11. Plot of first-order catalyst dependence for intramolecular hydroamination of **I** at different concentrations of **17** (■ = 4; ▼ = 6; ● = 8 mol%). Inset refers to the linearity of the observed *K* values versus catalyst concentration (see also the Supporting Information).

example of thermally stable, unsymmetrical Group IV metal complexes stabilized by dianionic N,C,N′ pincer ligands reported to date. In addition, only a few classes of Group IV pincer-type complexes have been reported as active systems in hydroamination reactions, all of them typically requiring severe reaction conditions.[37] The ability of our neutral amido systems to promote the intramolecular hydroamination reaction of model primary aminoalkenes (thus providing, for selected substrates, fast and complete conversion at room temperature) constitutes a remarkable step forward toward catalytic systems that can operate at relatively low catalyst loading (5 mol%) and under milder (time and temperature) reaction conditions. Preliminary kinetic investigations and substrate scope studies, in conjunction with DFT calculations on the real systems, have been used to elucidate the effects of the substrate substitution on the catalyst performance and to support the most reliable mechanistic path operative in the hydroamination reaction.

All these findings taken together pave the way to the future development of original N,C,N′ pincer-type early-transition-metal complexes based on C_1 symmetric ligands for the investigation of stereoselective hydroamination processes.

Experimental Section

General: All air- and/or moisture-sensitive reactions were performed in an inert atmosphere in flame-dried flasks by using standard Schlenk-type techniques or in a dry-box filled with nitrogen. Anhydrous toluene, THF, and Et_2O were obtained by means of a MBraun solvent purification system, whereas CH_2Cl_2 and MeOH were distilled over CaH_2 and Mg, respectively. Unless otherwise stated, all the other reagents and solvents were used as purchased from commercial suppliers. (3-Bromophenyl)hydrazine (**5**) was straightforwardly obtained from crystalline (3-bromophenyl)hydrazine hydrochloride upon washing with an aqueous NaOH solution (30% w/w) and successive extraction in benzene.[38] Ethyl 2-[(dimethylamino)methylene]-3-oxobutanoate (**6**) was prepared on a multigram scale according to reported procedures.[20] [D_6]Benzene and [D_8]toluene were dried over sodium/benzophenone ketyl and condensed in vacuo over activated 4 Å molecular sieves prior to use. 1D (^{1}H and ^{13}C{^{1}H}) and 2D (COSY H,H; HETCOR H,C) NMR spectra of all the organometallic species were obtained on either a Bruker Avance DRX-400 spectrometer (400.13 and 100.61 MHz for ^{1}H and ^{13}C, respectively) or a Bruker Avance 300 MHz instrument (300.13 and 75.47 MHz for ^{1}H and ^{13}C, respectively). Chemical shifts are reported in ppm (δ) relative to TMS, referenced to the chemical shifts of residual solvent resonances (^{1}H and ^{13}C). The multiplicities of the ^{13}C{^{1}H} NMR spectra were determined on the basis of the ^{13}C{^{1}H} JMOD sequence and quoted as: CH_3, CH_2, CH, and C for primary, secondary, tertiary, and quaternary carbon atoms, respectively. The C, H, N, S elemental analyses were made at ICCOM-CNR using a Thermo FlashEA 1112 Series CHNS-O elemental analyzer with an accepted tolerance of ±0.4 units on carbon (C), hydrogen (H), and nitrogen (N).

X-ray data measurements: Single-crystal X-ray data were collected at low temperature (100 or 120 K) on an Oxford Diffraction XCALIBUR 3 diffractometer equipped with a CCD area detector using $Mo_{K\alpha}$ radiation (λ = 0.7107 Å).[52] The program used for the data collection was CrysAlis CCD1.171.[39] Data reduction was carried out with the program CrysAlis RED1.171[40] and the absorption correction was applied with the program ABSPACK1.17. Direct methods implemented in Sir97[41] were used to solve the structures and the refinements were performed by full-matrix least-squares against F^2 implemented in SHELX97.[42] All the non-hydrogen atoms were refined anisotropically, and the hydrogen atoms were fixed in calculated positions and refined isotropically with the thermal factor depending on the one of the atoms to which they are bound (riding model). Disorder on the $-NMe_2$ substituents in **19** and **20** was not explicitly treated because this process did not lead to a significant improvement of the structural final *R* factors. Molecular plots were produced by the program ORTEP3.[43] GC analyses of the reaction products were performed on a Shimadzu GC-17 gas chromatograph equipped with a flame ionization detector and a Supelco SPB-1 fused silica capillary column (length: 30 m, i.d.: 0.25 mm, film thickness: 0.25 μm) or a HP-PLOT Al_2O_3 KCl column (length: 50 m, i.d.: 0.53 mm, film thickness: 15 μm). The GC-MS analyses were performed on a Shimadzu QP2010S apparatus equipped with a column identical to that used for the GC analysis.

Synthesis of *N*-(3-bromobenzylidene)-2,6-diisopropylaniline (2): A solution of 3-bromobenzaldehyde (0.945 mL, 8.1 mmol), 2,6-diisopropylaniline (2.29 mL, 12.15 mmol), and 4-toluensulfonic acid (0.230 g, 1.21 mmol) in distilled toluene (40 mL) was maintained at reflux for 12 h in a Dean–Stark apparatus. The reaction mixture was allowed to cool to room temperature and then treated with 0.5 M aqueous NaOH solution (15 mL). The formed layers were separated and the aqueous phase was extracted with EtOAc (3× 15 mL). The combined organic extracts were dried over Na_2SO_4. After removal of the solvent under reduced pressure, a crude yellow oil was obtained. The pure product was finally precipitated by the addition of cold hexane (−20 °C), and yellow crystals were separated off by filtration. The collected crystals were washed with cold hexane and dried in vacuum to constant weight (2.200 g, 78.8%). ^{1}H NMR (300 MHz, CD_2Cl_2, 293 K): δ = 1.19 (d, $^3J_{HH}$ = 6.9 Hz, 12H; CH(CH_3); H15, H16, H18, H19), 2.97 (sept, $^3J_{HH}$ = 6.9 Hz, 2H; C*H*(CH_3); H14, H17), 7.11–7.21 (3H; C*H* Ar; H10, H11, H12), 7.43 (m, 1H; C*H* Ar; H3), 7.70 (m, 1H; C*H*; H4), 7.86 (m, 1H; C*H* Ar; H2), 8.16–8.18 ppm (2H; H6, H7); ^{13}C{^{1}H} NMR (75 MHz, CD_2Cl_2, 293 K): δ = 23.2 (CH(CH_3)$_2$; C15, C16, C18, C19), 27.9 (*C*H(CH_3)$_2$; C14, C17), 122.9 (C5), 123.0 (C10, C12), 124.2 (C11), 127.4 (C2), 130.4 (C3), 130.9 (C6), 134.2 (C4), 137.4 (C9,13), 138.0 (C8), 148.8 (C1), 160.5 ppm (C7); elemental analysis (%) calcd for $C_{19}H_{22}BrN$ (344.29): C 66.28, H 6.44, N 4.07; found: C 66.15, H 6.38, N 4.33.

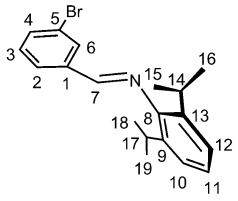

Synthesis of *N*-(3-bromobenzyl)-2,6-diisopropylaniline (3): $NaBH_3CN$ (0.54 g, 8.71 mmol) and acetic acid (0.54 mL, 8.71 mmol) were added in sequence to a

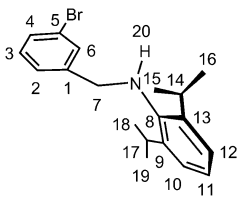

© 2013 Wiley-VCH Verlag GmbH & Co. KGaA, Weinheim

These are not the final page numbers!

cooled (0 °C) solution of **2** (2.00 g, 5.80 mmol) in dry and degassed MeOH/THF (1:1, 36 mL) in a nitrogen atmosphere. The reaction temperature was raised to 50 °C, and the resulting mixture was stirred at the same temperature for 2 h. Afterwards, the reaction mixture was allowed to cool to room temperature and a mixture of saturated Na_2CO_3 and water (1:1, 40 mL) was added in one portion. The organic phase was separated and the aqueous layer was extracted with EtOAc (3×20 mL). The collected organic layers were dried over Na_2SO_4 and the residue was purified by flash chromatography on silica gel with petroleum ether/EtOAc (95:5) as the eluent to give the pure product **3** as white crystals (1.95 g, 97%). ^{1}H NMR (300 MHz, CD_2Cl_2, 293 K): δ=1.26 (d, $^3J_{HH}$=6.8 Hz, 12H; CH(CH_3); H15, H16, H18, H19), 3.21 (brs, 1H; N*H*; H20), 3.32 (sept, $^3J_{HH}$=6.8 Hz, 2H; C*H*(CH_3); H14, H17), 4.05 (s, 1H; CH_2NH; H7), 7.09–7.18 (3H; C*H* Ar; H10, H11, H12), 7.29 (m, 1H; C*H* Ar; H3), 7.41 (m, 1H; C*H*; H2), 7.48 (m, 1H; C*H* Ar; H4), 7.65 ppm (m, 1H; C*H* Ar; H6); ^{13}C{^{1}H} NMR (75 MHz, CD_2Cl_2, 293 K): δ=24.0 (CH(CH_3)$_2$; C15, C16, C18, C19), 27.6 (*C*H(CH_3)$_2$; C14, C17), 55.3 (C7), 122.4 (C5), 123.5 (C10, C12), 124.2 (C11), 126.5 (C2), 130.1 (C3), 130.2 (C4), 130.7 (C6), 142.5 (C1), 142.7 (C8), 143.0 ppm (C9, C13); elemental analysis (%) calcd for $C_{19}H_{24}BrN$ (346.30): C 65.90, H 6.99, N 4.04; found: C 65.85, H 6.94, N 4.16.

Synthesis of *N*-[3-(1*H*-pyrazol-1-yl)benzyl]-2,6-diisopropylaniline (H_2L; 4): Potassium carbonate (0.32 g, 2.30 mmol); copper(I) iodide (0.022 g, 0.11 mmol), and pyrazole (0.082 g, 1.21 mmol) were added to a solution of **3** (0.400 mL, 1.15 mmol) in NMP (7 mL). The reaction mixture was heated in a N_2 atmosphere at 210 °C for 5 h using microwave irradiation on a CEM Discover apparatus operating at 250 W. Afterwards, the reaction mixture was cooled to room temperature, filtered over a celite pad, and washed with EtOAc. The filtrate was evaporated under vacuum and the residue was purified by flash chromatography on silica gel with petroleum ether/EtOAc (92:8) as the eluent to give the final product **4** as off-white crystals (0.340 g, 88.5%). ^{1}H NMR (300 MHz, CD_2Cl_2, 293 K): δ=1.37 (d, $^3J_{HH}$=6.8 Hz, 12H; CH(CH_3); H15, H16, H18, H19), 3.44–3.53 (2H; H14, H17, H20), 4.25 (s, 1H; CH_2NH; H7), 6.57 (m, 1H; C*H* Ar; H22), 7.19–7.29 (3H; C*H* Ar; H10, H11, H12), 7.48–7.57 (2H; C*H* Ar; H3, H2), 7.76 (m, 1H; C*H* Ar; H4), 7.83 (m, 1H; C*H* Ar; H23), 7.97 (m, 1H; C*H* Ar; H6), 8.08 ppm (d, $^3J_{HH}$=2.4 Hz, 1H; C*H* Ar; H21); ^{13}C{^{1}H} NMR (75 MHz, CD_2Cl_2, 293 K): δ=24.2 (CH(CH_3)$_2$; C15, C16, C18, C19), 27.8 (*C*H(CH_3)$_2$; C14, C17), 55.8 (C7), 117.8 (C4), 118.3 (C6), 123.7 (C10, C12), 124.3 (C11), 125.7 (C2), 126.8 (C21), 129.5 (C3), 140.4 (C5), 141.0 (C23), 142.1 (C8), 142.9 (C1), 143.1 ppm (C9, C13); elemental analysis (%) calcd for $C_{22}H_{27}N_3$ (333.47): C 79.24, H 8.16, N 12.60; found: C 79.19, H 8.14, N 12.67.

Synthesis of ethyl 1-(3-bromophenyl)-5-methyl-1*H*-pyrazole-4-carboxylate (7): (3-Bromophenyl)hydrazine (0.700 g, 3.74 mmol) in ethanol (7.5 mL) was added dropwise to ethyl 2-[(dimethylamino)methylene]-3-oxobutanoate (0.660 g, 3.56 mmol) in ethanol (7.5 mL). The resulting solution was heated to reflux for 2 h and evaporated under reduced pressure. The crude residue was diluted with water (15 mL) and extracted with chloroform (2×15 mL). The chloroform extracts were washed with a saturated solution of $NaHCO_3$ (3×15 mL) and with water, dried over Na_2SO_4, and evaporated under reduced pressure to give a crude yellow oil that was purified by flash chromatography on silica gel with petroleum ether/EtOAc (90:10) as the eluent to give pure **7** as orange crystals (0.960 g, 87.2%). ^{1}H NMR (300 MHz, CD_2Cl_2, 293 K): δ=1.35 (t, $^3J_{HH}$=7.1 Hz, 3H; CH_2CH_3; H13), 2.56 (s, 3H; CH_3; H10), 4.29 (q, $^3J_{HH}$=7.1 Hz, 2H; CH_2CH$_3$; H12), 7.38–7.40 (2H; H2, H3), 7.58–7.63 (2H; H4, H6), 7.98 ppm (s, 1H; C*H* Ar; H9); ^{13}C{^{1}H} NMR (75 MHz, CD_2Cl_2, 293 K): δ=11.7 (C10), 14.1 (CH_2CH_3; C13), 59.9 (CH_2CH_3; C12), 113.3 (C8), 122.4 (C5), 123.9 (C2), 128.4 (C6), 130.4 (C3), 131.4 (C4), 140.1 (C1), 141.9 (C9), 143.5 (C7), 163.4 ppm (C11); elemental analysis (%) calcd for $C_{13}H_{13}BrN_2O_2$ (309.16): C 50.50, H 4.24, N 9.06; found: C 50.47, H 4.22, N 9.14.

Synthesis of 1-(3-bromophenyl)-5-methyl-1*H*-pyrazole-4-carboxylic acid (8): LiOH (0.976 g, 23.28 mmol) was added in one portion to a solution of **7** (0.900 g, 2.91 mmol) in ethanol/water (8:2, 40 mL). The resulting solution was stirred at 80 °C for 16 h and then cooled to room temperature. The ethanol was evaporated under reduced pressure and the resulting mixture was diluted with water (10 mL). Afterwards, the solution pH value was adjusted to pH 4 by using a few drops of AcOH and the resulting mixture was extracted with CH_2Cl_2 (2×10 mL). The organic layers were combined, dried over Na_2SO_4, and evaporated under reduced pressure to give crude **8** as a white solid. The as-prepared material was not purified further and was directly used in the subsequent step (0.783 g, 95.7%). ^{1}H NMR (300 MHz, $CDCl_3$, 293 K): δ=2.59 (s, 3H; CH_3; H10), 7.36–7.38 (2H; H2, H3), 7.57–7.62 (2H; H4, H6), 8.09 ppm (s, 1H; C*H* Ar; H9); ^{13}C{^{1}H} NMR (75 MHz, $CDCl_3$, 293 K): δ=12.0 (C10), 112.5 (C8), 122.7 (C5), 124.0 (C2), 128.7 (C6), 130.5 (C3), 131.9 (C4), 139.7 (C1), 142.9 (C9), 144.7 (C7), 169.0 ppm (C11).

Synthesis of 1-(3-bromophenyl)-5-methyl-1*H*-pyrazole (9): Carboxylic acid **9** (0.300 g, 1.06 mmol) was collected in a sealed glass vial in an inert atmosphere and heated at 215 °C for 60 h. The resulting brown oil was purified by flash chromatography on silica gel with petroleum ether/EtOAc as the eluent (80:20) to give the pure product **9** as a colorless oil (0.234 g, 93%). ^{1}H NMR (300 MHz, CD_2Cl_2, 293 K): δ=2.39 (s, 3H; CH_3; H10), 6.23 (m, 1H; C*H* Ar; H8), 7.36–7.47 (2H; H2, H3), 7.53–7.56 (2H; H4, H9), 7.70 ppm (m, 1H; C*H* Ar; H6); ^{13}C{^{1}H} NMR (75 MHz, CD_2Cl_2, 293 K): δ=12.3 (C10), 107.3 (C8), 122.3 (C5), 123.0 (C2), 127.6 (C6), 130.2 (C3, C4), 138.8 (C1), 140.1 (C9), 141.2 ppm (C7); elemental analysis (%) calcd for $C_{10}H_9BrN_2$ (237.10): C 50.66, H 3.83, N 11.82; found: C 50.70, H 3.85, N 11.84.

Synthesis of 3-(5-methyl-1*H*-pyrazol-1-yl)benzaldehyde (10): A suspension of **9** (0.360 g, 1.52 mmol) and sodium formate (0.133 g, 2.28 mmol) in dry DMF (4 mL) was treated with bis(triphenylphosphine)palladium(II) chloride (0.045 g, 0.07 mmol). CO was gently bubbled through the suspension with a teflon cannula and the mixture was stirred at 110 °C for 1 h. After cooling, the mixture was treated with an aqueous Na_2CO_3 solution and extracted with EtOAc (3×30 mL). The collected organic layers were dried over Na_2SO_4 and evaporated under reduced pressure to give a crude semisolid material. Purification by flash chromatography on silica gel with petroleum ether/EtOAc (80:20) as the eluent gave the pure **10** as a pale-yellow oil (0.235 g, 83%). ^{1}H NMR (300 MHz, CD_2Cl_2, 293 K): δ=2.34 (s, 3H; CH_3; H10), 6.18 (m, 1H; C*H* Ar; H8), 7.51 (m, 1H; C*H* Ar; H9), 7.69 (m, 1H; C*H* Ar; H3), 7.71 (m, 1H; C*H* Ar; H4), 7.81 (m, 1H; C*H* Ar; H2), 7.91 (m, 1H; C*H* Ar; H6), 10.00 ppm (s, 1H; C*H*O; H11); ^{13}C{^{1}H} NMR (75 MHz, CD_2Cl_2, 293 K): δ=12.3 (C10), 107.4 (C8), 124.8 (C6), 128.1 (C2), 129.9 (C3, C4), 137.3 (C5), 138.9 (C7), 140.2 (C9), 140.8 (C1), 191.2 ppm (C11); elemental analysis (%) calcd for $C_{11}H_{10}N_2O$ (186.21): C 70.95, H 5.41, N 15.04; found C 70.92, H 5.43, N 15.09.

Synthesis of 2,6-diisopropyl-*N*-[3-(5-methyl-1*H*-pyrazol-1-yl)benzylidene]aniline (11): A solution of the benzaldehyde **10** (0.170 g, 0.9 mmol) in distilled toluene (10 mL) was treated with 2,6-diisopropylaniline (0.26 mL, 1.37 mmol) and 4-toluensulfonic acid (0.02 g, 0.13 mmol). The resulting solution was heated to reflux for 12 h in a Dean–Stark apparatus. Afterwards, the reaction mixture was cooled to room temperature and treated with aqueous 0.5 M NaOH solution (5 mL). The formed layers were separated and the aqueous

© 2013 Wiley-VCH Verlag GmbH & Co. KGaA, Weinheim

phase was washed with EtOAc (3×10 mL). The collected organic extracts were dried over Na_2SO_4, and the solvent was evaporated under reduced pressure to give a crude yellow oil. The pure product was finally precipitated from cold hexane (−20 °C) in the form of pure yellow crystals. The latter were separated by filtration and washed with cold hexane (0.295 g, 93.6 %). ^{1}H NMR (300 MHz, CD_2Cl_2, 293 K): δ = 1.20 (d, $^3J_{HH}$ = 6.8 Hz, 12H; CH(CH_3); H19, H20, H22, H23), 2.46 (s, 3H; CH_3; H10), 3.00 (sept, $^3J_{HH}$ = 6.8 Hz, 2H; CH(CH$_3$); H18, H21), 6.28 (m, 1H; CH; H8), 7.11–7.15 (m, 1H; CH Ar; H15), 7.19–7.21 (2H; CH Ar; H14, H16), 7.61 (m, 1H; CH Ar; H9), 7.65–7.66 (2H; CH Ar; H2, H3), 7.94–7.96 (m, 1H; CH Ar; H4), 8.06 (m, 1H; H6), 8.26 ppm (s, 1H; CHN; H11); ^{13}C(^{1}H) NMR (75 MHz, CD_2Cl_2, 293 K): δ = 12.3 (C10), 23.1 (CH-(CH_3)$_2$; C19, C20, C22, C23), 27.9 (CH(CH$_3$)$_2$; C18, C21), 107.2 (C8), 122.9 (C14, C16), 124.1 (C6, C15), 127.1 (C2), 127.4 (C4), 129.4 (C3), 137.1 (C5), 137.4 (C13, H17), 138.8 (C7), 140.0 (C9), 140.6 (C1), 149.0 (C12), 161.1 ppm (C11); elemental analysis (%) calcd for $C_{23}H_{27}N_3$ (345.48): C 79.96, H 7.88, N 12.16; found: C 80.00, H 7.93, N 12.07.

Synthesis of 2,6-diisopropyl-*N*-[3-(5-methyl-1*H*-pyrazol-1-yl)benzyl]aniline (H_2L^{Me}) (12): $NaBH_3CN$ (0.06 g, 1.02 mmol) and acetic acid (0.06 mL, 1.02 mmol) were added in sequence to a cooled solution (0 °C) of **11** (0.295 g, 0.85 mmol) in dry, degassed MeOH/THF (1:1, 5 mL). The resulting mixture was maintained under stirring and in an inert atmosphere at room temperature for 1 h. Afterwards, saturated Na_2CO_3 and water (1:1) were added, the organic phase was separated, and the aqueous layer was extracted with EtOAc (3×10 mL). The collected organic layers were dried over Na_2SO_4, and the solvent was evaporated under reduced pressure. The crude residue was purified by flash chromatography on silica gel with petroleum ether/EtOAc (83:17) as the eluent to give the pure product **12** as a colorless oil (0.272 g, 92.0 %). ^{1}H NMR (300 MHz, CD_2Cl_2, 293 K): δ = 1.30 (d, $^3J_{HH}$ = 6.8 Hz, 12H; CH(CH_3); H19, H20, H22, H23), 2.41 (s, 3H; CH_3; H10), 3.33–3.45 (3H; CH(CH$_3$), NH; H18, H21, H24), 4.18 (s, 1H; CH_2NH; H11), 6.28 (m, 1H; CH; H8), 7.12–7.21 (3H; CH Ar; H14, H15, H16), 7.43–7.54 (3H; CH Ar; H2, H3, H4), 7.61–7.63 ppm (2H; CH Ar; H9, H6); ^{13}C{^{1}H} NMR (75 MHz, CD_2Cl_2, 293 K): δ = 12.3 (C10), 24.1 (CH-(CH_3)$_2$; C19, C20, C22, C23), 27.7 (CH(CH$_3$)$_2$; C18, C21), 55.6 (C11), 106.9 (C8), 123.4 (C2), 123.6 (C14, C16), 124.0 (C6), 124.2 (C15), 126.8 (C4), 129.0 (C3), 138.7 (C7), 139.6 (C9), 140.2 (C1), 141.6 (C12), 142.7 (C5), 143.0 ppm (C13, C17); elemental analysis (%) calcd for $C_{23}H_{29}N_3$ (347.50): C 79.50, H 8.41, N 12.09; found: C 79.55, H 8.43, N 12.02.

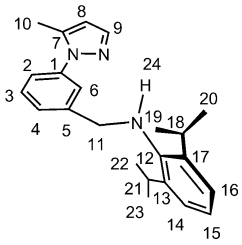

General procedure for the synthesis of complexes [Zr^{IV}(κ-*N*-HL)-(NMe_2)$_3$] (13), [Hf^{IV}(κ-*N*-HL)(NMe_2)$_3$] (14), [Zr^{IV}(κ-*N*-HL^{Me})(NMe_2)$_3$] (15), and [Hf^{IV}(κ-*N*-HL^{Me})(NMe_2)$_3$] (16): A solution of the selected ligands H_2L **4** or H_2L^{Me} **12** (1 mmol) in dry and degassed benzene (4 mL) was treated dropwise with a solution of the proper metal precursor ([M^{IV}-(NMe_2)$_4$] 99 %; M = Zr, Hf; 1.05 equiv) in benzene (3 mL). The reaction mixture was maintained under stirring at room temperature for 20 h and then concentrated in vacuo to afford semisolid pale-yellow crude materials. The purification of **13** and **14** was conveniently achieved by crystallization from concentrated solutions of the complexes in pentane cooled at −30 °C, thus yielding pale-yellow and white crystals, respectively, suitable for X-ray diffraction analyses (94 % yield of the isolated products). Complexes **15** and **16** were obtained as pale-yellow oils, and all attempts to isolate crystals failed. However, both complexes were analytically pure with no traces of residual reagents/solvents. These oils were dried under vacuum to constant weight.

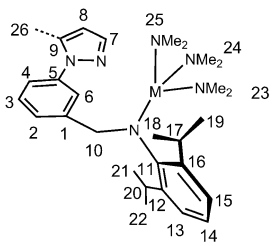

13: (96 % yield of isolated product); ^{1}H NMR (300 MHz, CD_2Cl_2, 293 K): δ = 1.06 (d, $^3J_{HH}$ = 6.9 Hz, 6H; CH(CH$_3^A$CH_3^B); H19, H22), 1.16 (d, $^3J_{HH}$ = 6.9 Hz, 6H; CH(CH_3^ACH$_3^B$); H18, H21), 2.75 (brs, 18H; N(CH_3)$_2$; H23, H24, H25), 3.50 (sept, $^3J_{HH}$ = 6.9 Hz, 2H; CH(CH$_3$)$_2$; H17, H20), 4.44 (s, 2H; CH_2N; H10), 6.48 (m, 1H; CH Ar; H8), 7.12–7.15 (4H; CH Ar; H2, H13, H14, H15), 7.38 (t, $^3J_{HH}$ = 7.8 Hz, 1H; CH Ar; H3), 7.47 (m, 1H; CH Ar; H6), 7.60 (m, 1H; CH Ar; H4), 7.70 (m, 1H; CH Ar; H7), 7.85 ppm (m, 1H; CH Ar; H9); ^{13}C{^{1}H} NMR (75 MHz, CD_2Cl_2, 293 K): δ = 24.0 (CH(CH$_3^A$CH$_3^B$); C18, C21), 25.0 (CH(CH$_3^A$CH$_3^B$); C19, C22), 27.7 (CH(CH$_3$)$_2$; C17, C20), 41.0 (N(CH$_3$); C23, C24, C25), 60.4 (C10), 107.3 (C8), 117.7 (C4), 120.1 (C6), 123.7 (C13, C15), 124.9 (C14), 126.5 (C9), 127.6 (C2), 129.1 (C3), 140.7 (C7), 142.7 (C), 143.0 (C), 144.0 (C), 147.8 ppm (C12, C16); elemental analysis (%) calcd for $C_{28}H_{44}N_6Zr$ (555.91): C 60.49, H 7.98, N 15.12; found: C 60.52, H 8.03, N 15.10.

14: (94 % yield of isolated product); ^{1}H NMR (300 MHz, CD_2Cl_2, 293 K): δ = 1.05 (d, $^3J_{HH}$ = 6.9 Hz, 6H; CH(CH$_3^A$CH$_3^B$); H19, H22), 1.17 (d, $^3J_{HH}$ = 6.9 Hz, 6H; CH(CH_3^ACH$_3^B$); H18, H21), 2.78 (brs, 18H; N(CH_3)$_2$; H23, H24, H25), 3.52 (sept, $^3J_{HH}$ = 6.9 Hz, 2H; CH(CH$_3$)$_2$; H17, H20), 4.50 (s, 2H; CH_2N; H10), 6.48 (m, 1H; CH Ar; H8), 7.10–7.14 (4H; CH Ar; H2, H13, H14, H15), 7.38 (t, $^3J_{HH}$ = 7.8 Hz, 1H; CH Ar; H3), 7.44 (m, 1H; CH Ar; H6), 7.70 (m, 1H; CH Ar; H4), 7.70 (m, 1H; CH Ar; H7), 7.84 ppm (m, 1H; CH Ar; H9); ^{13}C{^{1}H} NMR (75 MHz, CD_2Cl_2, 293 K): δ = 24.0 (CH(CH$_3^A$CH$_3^B$); C18, H21), 25.0 (CH(CH$_3^A$CH$_3^B$); C19, H22), 27.7 (CH(CH$_3$)$_2$; C17, H20), 40.6 (N(CH$_3$); C23, H24, H25), 60.0 (C10), 107.3 (C8), 117.7 (C4), 120.2 (C6), 123.7 (C13, H15), 125.0 (C14), 126.5 (C9), 127.6 (C2), 129.1 (C3), 140.0 (C), 140.7 (C7), 142.6 (C), 143.9 (C), 147.9 (C12, H16); elemental analysis (%) calcd for $C_{28}H_{44}N_6Hf$ (643.18): C 52.29, H 6.90, N 13.07; found: C 52.34, H 6.95, N, 13.00.

15: (95 % yield of isolated product); ^{1}H NMR (400 MHz, CD_2Cl_2, 293 K): δ = 1.02 (d, $^3J_{HH}$ = 6.9 Hz, 6H; CH(CH$_3^A$CH$_3^B$); H19, H22), 1.17 (d, $^3J_{HH}$ = 6.9 Hz, 6H; CH(CH_3^ACH$_3^B$); H18, H21), 2.19 (s, 3H; CH_3; H26), 2.79 (brs, 18H; N(CH_3)$_2$; H23, H24, H25), 3.48 (sept, $^3J_{HH}$ = 6.9 Hz, 2H; CH(CH$_3$)$_2$; H17, H20), 4.51 (s, 2H; CH_2N; H10), 6.18 (m, 1H; CH Ar; H8), 7.11 (brs, 3H; CH Ar; H13, H14, H15), 7.18 (brs, 1H; CH Ar; H6), 7.26 (m, 1H; CH Ar; H2), 7.33 (m, 1H; CH Ar; H4), 7.39–7.44 (1H; CH Ar; H3), 7.52 ppm (m, 1H; CH Ar; H7). ^{13}C{^{1}H} NMR (100 MHz, CD_2Cl_2, 293 K): δ 12.0 (CH$_3$; C26), 24.0 (CH(CH$_3^A$CH$_3^B$); C18, C21), 24.9 (CH(CH$_3^A$CH$_3^B$); C19, C22), 27.7 (CH(CH$_3$)$_2$; C17, C20), 41,1 (N-(CH$_3$); C23, C24, C25), 60.0 (C10), 106.6 (C8), 123.0 (C4), 123.7 (C13, C15), 125.0 (C14), 125.7 (C6), 128.2 (C2), 128.7 (C3), 138.5 (C9), 139.4 (C7), 139.8 (C), 142.2 (C), 143.5 (C), 147.8 ppm (C12, C16); elemental analysis (%) calcd for $C_{29}H_{46}N_6Zr$ (569.94): C 61.11, H 8.14, N 14.75; found: C 61.15, H 8.17, N 14.71.

16: (91 % yield of isolated product); ^{1}H NMR (400 MHz, CD_2Cl_2, 293 K): δ = 0.97 (d, $^3J_{HH}$ = 6.9 Hz, 6H; CH(CH$_3^A$CH$_3^B$); H19, H22), 1.13 (d, $^3J_{HH}$ = 6.9 Hz, 6H; CH(CH_3^ACH$_3^B$); H18, H21), 2.13 (s, 3H; CH_3; H26), 2.77 (brs, 18H; N(CH_3)$_2$; H23, H24, H25), 3.45 (sept, $^3J_{HH}$ = 6.9 Hz, 2H; CH(CH$_3$)$_2$; H17, H20), 4.50 (s, 2H; CH_2N; H10), 6.14 (m, 1H; CH Ar; H8), 7.07 (brs, 3H; CH Ar; H13, H14, H15), 7.11 (brs, 1H; CH Ar; H6), 7.19 (m, 1H; CH Ar; H2), 7.29 (m, 1H; CH Ar; H4), 7.35–7.39 (1H; CH Ar; H3), 7.48 ppm (m, 1H; CH Ar; H7); ^{13}C{^{1}H} NMR (100 MHz, CD_2Cl_2, 293 K): δ = 12.0 (CH$_3$; C26), 24.0 (CH(CH$_3^A$CH$_3^B$); C18, C21), 24.9 (CH(CH$_3^A$CH$_3^B$); C19, C22), 27.7 (CH(CH$_3$)$_2$; C17, C20), 40.6 (N-(CH$_3$); C23, C24, C25), 59.5 (C10), 106.6 (C8), 123.1 (C4), 123.7 (C13, C15), 125.0 (C14), 125.7 (C6), 128.7 (C2), 128.8 (C3), 138.5 (C9), 139.4 (C7), 139.8 (C), 142.1 (C), 143.5 (C), 147.9 ppm (C12, C16); elemental analysis (%) calcd for $C_{29}H_{46}N_6Hf$ (657.21): C 53.00, H 7.05, N 12.79; found: C 53.07, H 7.11, N 12.82.

General procedure for the synthesis of complexes [Zr^{IV}(κ^3-*N*,*C*,*N*-L)-(NMe_2)$_2$] (17), [Hf^{IV}(κ^3-*N*,*C*,*N*-L)(NMe_2)$_2$] (18), [Zr^{IV}(κ-*N*,*C*,*N*-L^{Me})-(NMe_2)$_2$] (19), and [Hf^{IV}(κ-*N*,*C*,*N*-L^{Me})(NMe_2)$_2$] (20): A solution of the selected ligands H_2L **4** or H_2L^{Me} **12** (1 mmol) in dry and degassed xylene

© 2013 Wiley-VCH Verlag GmbH & Co. KGaA, Weinheim

These are not the final page numbers!

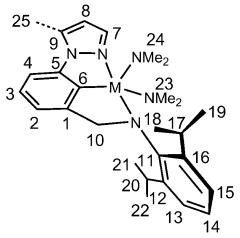

(4 mL) was treated dropwise with a solution of the proper metal precursor ([M^{IV}-$(NMe_2)_4$] 99%; M = Zr, Hf; 1.05 equiv) in xylene (4 mL). The reaction mixture was maintained under stirring at reflux for the appropriate reaction time until completeness (Table 3). Evaporation of the solvent under vacuum afforded the crude cyclometallated species as either dark-yellow or pale-yellow (Zr^{IV} and Hf^{IV} derivatives, respectively) microcrystals. Purification of the complexes was achieved by crystallization from concentrated toluene/pentane (1:1 v/v) cooled at −30 °C. Crystals suitable for X-ray diffraction analyses were obtained from each sample.

17: (87% yield of the isolated product); ^{1}H NMR (400 MHz, CD_2Cl_2, 293 K): δ = 1.15 (d, $^3J_{HH}$ = 6.9 Hz, 6H; CH($CH_3^ACH_3^B$); H19, H22), 1.21 (d, $^3J_{HH}$ = 6.9 Hz, 6H; CH($CH_3^ACH_3^B$); H18, H21), 2.73 (s, 12H; N-(CH_3)$_2$; H23, H24), 3.66 (sept, $^3J_{HH}$ = 6.9 Hz, 2H; C*H*(CH_3)$_2$; H17, H20), 4.71 (s, 2H; CH_2N; H10), 6.61 (m, 1H; C*H* Ar; H8), 7.06–7.18 (5H; C*H* Ar; H2, H4, H13, H14, H15), 7.24 (t, $^3J_{HH}$ = 7.8 Hz, 1H; C*H* Ar; H3), 7.78 (d, $^3J_{HH}$ = 2.1 Hz, 1H; C*H* Ar; H7), 8.13 ppm (d, $^3J_{HH}$ = 2.5 Hz, 1H; C*H* Ar; H9); 13C(^{1}H) NMR (100 MHz, CD_2Cl_2, 293 K): δ = 24.0 (CH($CH_3^ACH_3^B$); C18, C21), 26.0 (*C*H($CH_3^ACH_3^B$); C19, C22), 27.3 (*C*H(CH_3)$_2$; C17, C20), 39.9 (N(*C*H$_3$); C23, C24), 68.8 (C10), 107.0 (C4), 108.0 (C8), 121.2 (C2), 123.0 (C13, C15), 123.5 (C14), 125.7 (C9), 127.8 (C3), 140.5 (C7), 144.3 (C), 147.4 (C12, C16), 148.4 (C), 157.3 (C), 174.0 ppm (C6); elemental analysis (%) calcd for $C_{26}H_{37}N_5Zr$ (510.83): C 61.13, H 7.30, N 13.71: found: C 61.17, H 7.34, N 13.64.

18: (79% yield of the isolated product); ^{1}H NMR (400 MHz, CD_2Cl_2, 293 K): δ = 1.16 (d, $^3J_{HH}$ = 6.9 Hz, 6H; CH($CH_3^ACH_3^B$); H19, H22), 1.21 (d, $^3J_{HH}$ = 6.9 Hz, 6H; CH($CH_3^ACH_3^B$); H18, H21), 2.75 (s, 12H; N-(CH_3)$_2$; H23, H24), 3.68 (sept, $^3J_{HH}$ = 6.9 Hz, 2H; C*H*(CH_3)$_2$; H17, H20), 4.11 (s, 2H; CH_2N; H10), 6.60 (m, 1H; C*H* Ar; H8), 7.08 (m, 1H; CH Ar; H14), 7.10–7.17 (3H; C*H* Ar; H2, H13, H15), 7.23–7.26 (2H; CH Ar; H3, H4), 7.24 (t, $^3J_{HH}$ = 7.8 Hz, 1H; C*H* Ar; H3), 7.81 (d, $^3J_{HH}$ = 1.9 Hz, 1H; C*H* Ar; H7), 8.13 ppm (d, $^3J_{HH}$ = 2.5 Hz, 1H; C*H* Ar; H9); ^{13}C{^{1}H} NMR (100 MHz, CD_2Cl_2, 293 K): δ = 24.0 (CH($CH_3^ACH_3^B$); C18, C21), 26.0 (*C*H($CH_3^ACH_3^B$); C19, C22), 27.2 (*C*H(CH_3)$_2$; C17, C20), 39.7 (N(*C*H$_3$); C23, C24), 67.9 (C10), 107.2 (C4), 108.1 (C8), 121.6 (C2), 123.0 (C13, C15), 123.6 (C14), 126.1 (C9), 127.9 (C3), 140.7 (C7), 145.0 (C), 147.5 (C12, C16), 148.8 (C), 157.3 (C), 181.8 ppm (C6); elemental analysis (%) calcd for $C_{26}H_{37}N_5Hf$ (598.10): C 52.21, H 6.24, N 11.71; found: C 52.26, H 6.24, N 11.67.

19: (86% yield of the isolated product); ^{1}H NMR (400 MHz, CD_2Cl_2, 293 K): δ = 1.19 (d, $^3J_{HH}$ = 6.9 Hz, 6H; CH($CH_3^ACH_3^B$); H19. H22), 1.24 (d, $^3J_{HH}$ = 6.9 Hz, 6H; CH($CH_3^ACH_3^B$); H18, H21), 2.75 (s, 12H; N-(CH_3)$_2$; H23, H24), 2.79 (s, 3H; CH_3; H25) 3.70 (sept, $^3J_{HH}$ = 6.9 Hz, 2H; C*H*(CH_3)$_2$; H17, H20), 4.74 (s, 2H; CH_2N; H10), 6.35 (m, 1H; C*H* Ar; H8), 7.10–7.18 (4H; C*H* Ar; H2, H13, H14, H15), 7.25 (t, $^3J_{HH}$ = 7.8 Hz, 1H; C*H* Ar; H3), 7.33 (d, $^3J_{HH}$ = 7.8 Hz, 1H; C*H* Ar; H4), 7.68 ppm (m, 1H; C*H* Ar; H7); ^{13}C{^{1}H} NMR (100 MHz, CD_2Cl_2, 293 K): δ = 14.1 (*C*H$_3$; C25), 24.0 (CH($CH_3^ACH_3^B$); C18, C21), 26.1 (*C*H($CH_3^ACH_3^B$); C19, C22), 27.3 (*C*H(CH_3)$_2$; C17, C20), 40.0 (N(*C*H$_3$); C23, C24), 68.7 (C10), 109.1 (C4), 109.5 (C8), 120.9 (C2), 123.0 (C13, C15), 123.5 (C14), 127.7 (C3), 140.0 (C7), 140.3 (C9), 146.3 (C), 147.4 (C12, C16), 148.6 (C), 157.1 (C), 175.5 ppm (C6); elemental analysis (%) calcd for $C_{27}H_{39}N_5Zr$ (524.86): C 61.79, H 7.49, N 13.34; found: C 61.83, H 7.52, N 13.28.

20: (83% yield of the isolated product); ^{1}H NMR (400 MHz, CD_2Cl_2, 293 K): δ = 1.17 (d, $^3J_{HH}$ = 6.9 Hz, 6H; CH($CH_3^ACH_3^B$); H19, H22), 1.21 (d, $^3J_{HH}$ = 6.9 Hz, 6H; CH($CH_3^ACH_3^B$); H18, H21), 2.74 (s, 12H; N-(CH_3)$_2$; H23, H24), 2.79 (s, 3H; CH_3; H25) 3.68 (sept, $^3J_{HH}$ = 6.9 Hz, 2H; C*H*(CH_3)$_2$; H17, H20), 4.81 (s, 2H; CH_2N; H10), 6.32 (m, 1H; C*H* Ar; H8), 7.08 (m, 1H; C*H* Ar; H14), 7.14–7.16 (3H; C*H* Ar; H2, H13, H15), 7.24 (t, $^3J_{HH}$ = 7.8 Hz, 1H; C*H* Ar; H3), 7.37 (d, $^3J_{HH}$ = 7.8 Hz, 1H; C*H* Ar; H4), 7.69 ppm (m, 1H; C*H* Ar; H7); ^{13}C{^{1}H} NMR (100 MHz, CD_2Cl_2, 293 K): δ = 14.0 (*C*H$_3$; C25), 24.0 (CH($CH_3^ACH_3^B$); C18, C21), 26.0 (*C*H($CH_3^ACH_3^B$); C19, C22), 27.2 (*C*H(CH_3)$_2$; C17, C20), 39.7 (N-(*C*H$_3$); C23, C24), 67.8 (C10), 109.3 (C4), 109.5 (C8), 121.2 (C2), 122.9 (C13·15), 123.5 (C14), 127.8 (C3), 140.3 (C7), 140.7 (C9), 146.8 (C), 147.4 (C12·16), 149.1 (C), 157.1 (C), 183.1 ppm (C6); elemental analysis (%) calcd for $C_{27}H_{39}N_5Hf$ (612.12): C 52.98, H 6.42, N 11.44; found: C 53.02, H 6.43, N 11.39.

General procedure for intramolecular hydroamination of aminoalkenes I–V: All catalytic tests were set-up in an inert atmosphere in a N_2-filled drybox. The amido precursors **13**, **14**, and **17**–**20** were tested as neutral catalysts in the intramolecular hydroamination reaction in a two-necked 10 mL round-bottom flask equipped with a magnetic stirring bar, a glass stopper, and a septum. In a typical procedure, a solution of the catalyst (5 mol%) in dry and degassed benzene (1,5 mL; toluene was used for selected issues; Table 4) was treated in one portion with a solution of the aminoalkene (0.632 mmol) in dry and degassed benzene (0.5 mL) and ferrocene as an internal standard (0.2 mL of a stock 0.17 M ferrocene solution in benzene). Afterwards, the system was heated at the final temperature and the reaction course was periodically monitored by analyzing a samples of the mixture by GC-MS analysis until completeness or at fixed times. The conversion of the reaction was calculated by comparative integration of the product and substrate peak signals (on the ^{1}H NMR spectrum) with the internal standard peak (ferrocene). For selected issues, the reaction mixture was finally concentrated under reduced pressure and the crude material was purified by flash chromatography with CH_2Cl_2/MeOH (95:5) typically as the eluent to give the pure pyrrolidine product.

Kinetic measurements for 17 and 18: Kinetic studies were performed for the conversion of **I** at room temperature under optimized reaction conditions (Table 4, entries 4 and 19). Variable concentrations of the catalyst (4, 6, or 8 mol%) were also used for the best performing catalyst **17** at room temperature. All the measurements were carried out in a sealed J-Young NMR spectroscopic tube and the reaction course was monitored by ^{1}H NMR spectroscopic analysis recorded at constant times with ferrocene as an internal standard for the relative integration of the ^{1}H NMR signals. Comparison of the integration of product and substrate peaks with the internal-standard peaks was used to calculate the relative percentage of substrate and product at any given time. Both catalyst precursors **17** and **18** showed a first-order dependence in the substrate consumption/cyclization. In a typical procedure, stock solutions of catalyst precursors **17** and **18** were prepared by dissolving an aliquot (20 mg) of each complex in [D_6]benzene (0.5 mL). Compound **I** (20 mg, 0.084 mmol) and ferrocene (5 mg, 26.87 μmol; 98%)[15h] were weighted into a 1 mL volumetric flask and dissolved in [D_6]benzene (ca. 0.2 mL). Afterwards, a proper amount of the stock solution of the catalyst precursor (0.05 mL of **17**; 0.06 mL of **18**) was added to the volumetric flask, and the volume was topped to 1 mL with [D_6]benzene. The as-prepared solution was shaken and an aliquot of the solution (0.8 mL) was rapidly transferred into the J-Young NMR tube. The tube was placed into a 300 MHz NMR probe and acquisitions started immediately. For kinetic measurements carried out at 80 °C, a preheated 300 MHz NMR probe was used and the sample was allowed to thermally equilibrate for 2 min prior starting to collect the first ^{1}H NMR spectrum at $t = t_0$. The ^{1}H NMR spectra (8 scans) were collected every 5–10 min till the substrate conversion was almost complete (at least 90%).

Computational details: DFT geometry optimizations in the gas phase of the real systems **13** and **15** were performed using the Gaussian09 program (revision A.02).[44] The starting geometry for **13** was obtained from its XRD structure by rotating the phenylpyrazole fragment around the N1−C7 bond of about 180° (see main text for the atom numbering) to get a more suitable conformer for cyclometallation to occur. The starting geometry for **15** was obtained from the optimized structure of **13** by replacing the proton on C22 of the pyrazole ring with a methyl group. Both initial guesses were optimized with a M06 functional[45] by using the LANL2DZ pseudopotential[46] and related basis set[47] on the Zr atom and a 6–31G* basis set on all the other atoms. An extra *f*-type polarization function for the Zr center was added to the standard set.[47] Energetic profiles for the reaction pathways related to the hydroamination/cyclization of **I** and **III** catalyzed by **17** were simulated with the CP2K/Quickstep package by using a hybrid Gaussian and plane-wave method[48] within a DFT framework. A double-quality Gaussian basis-set plus polar-

© 2013 Wiley-VCH Verlag GmbH & Co. KGaA, Weinheim

ization function (DZVP) was employed for all the atoms. The Goedecker-Teter-Hutter pseudopotentials[49] together with a 320 Ry plane wave cutoff were used to expand the densities obtained with the Perdew-Burke-Ernzerhof (PBE)[50] exchange-correlation density functional. Van der Waals forces are taken in account with the Grimme D3 Method.[51] Molecular geometry optimization of stationary points used the Broyden-Fletcher-Goldfarb-Shanno (BFGS) method. The transition states were searched with the "distinguished-reaction-coordinate procedure" along the emerging bonds. Entropic and solvents effects for the cyclization process catalyzed by **17** and involving precursors **I** and **III** can be reasonably considered to be comparable, and their contribution have been omitted. Finally, incoming substrates involved in the protonolysis steps (see Figure 9 and Figure S40 (TS3 and TS4) in the Supporting Information) are modeled by adopting the simpler 1-aminopent-4-ene because only the amino termination is interested in the proton-transfer processes investigated.

Acknowledgements

The authors thank the Groupe de Recherche International (GDR1) "Homogeneous Catalysis for Sustainable Development" for support. We also acknowledge CINECA AwardN. HP10BD82EA 2011 for providing high-performance computing resources and support.

[1] For comprehensive reviews on pincer-type complexes and their application in catalysis, see: a) M. H. P. Rietveld, D. M. Grove, G. van Koten, *New J. Chem.* **1997**, *21*, 751; b) M. Albrecht, G. van Koten, *Angew. Chem.* **2001**, *113*, 3866; *Angew. Chem. Int. Ed.* **2001**, *40*, 3750; c) M. E. Van der Boom, D. Milstein, *Chem. Rev.* **2003**, *103*, 1759; d) J. T. Singleton, *Tetrahedron* **2003**, *59*, 1837; e) D. Morales-Morales, *Rev. Quim. Méx.* **2004**, *48*, 338; f) M. Q. Slagt, D. A. P. Zwieten, A. J. C. M. Moerkerk, R. J. M. K. Gebbink, G. van Koten, *Coord. Chem. Rev.* **2004**, *248*, 2275; g) D. Pugh, A. A. Danopoulos, *Coord. Chem. Rev.* **2007**, *251*, 610; h) D. Morales-Morales, C. M. Jensen in *The Chemistry of Pincer Compounds*, Elsevier Science, **2007**, pp. 450; i) J-L. Niu, X.-Q. Hao, J.-F. Gong, M.-P. Song, *Dalton Trans.* **2011**, *40*, 5135; j) N. Selander, K. J. Szabó, *Chem. Rev.* **2011**, *111*, 2048.

[2] G. van Koten, J. T. B. H. Jastrzebski, J. G. Noltes, A. L. Spek, J. C. Schoone, *J. Organomet. Chem.* **1978**, *148*, 233.

[3] For selected examples of mono- and trianionic N,C,N-pincer complexes with early transition metals, see: a) J. G. Donkervoort, J. T. B. H. Jastrzebski, B.-J. Deelman; H. Kooijman, N. Veldman, A. L. Spek, G. van Koten, *Organometallics* **1997**, *16*, 4174; H. Kooijman, N. Veldman, A. L. Spek, G. van Koten, *Organometallics* **1997**, *16*, 4174; b) M. Contel, M. Stol, M. A. Casado, G. P. M. van Klink, D. D. Ellis, A. L. Spek, G. van Koten, *Organometallics* **2002**, *21*, 4556; c) J. Koller, S. Sarkar, K. A. Abboud, A. S. Veige, *Organometallics* **2007**, *26*, 5438; d) S. Sarkar, K. P. McGowan, J. A. Culver, A. R. Carloson, J. Koller, A. J. Peloquin, M. K. Veige, K. A. Abboud, A. S. Veige, *Inorg. Chem.* **2010**, *49*, 5143; e) A. V. Chuchuryukin, R. Huang, M. Lutz, J. C. Chadwick, A. L. Spek, G. van Koten, *Organometallics* **2011**, *30*, 2819; f) A. V. Chuchuryukin, R. Huang, E. E. van Faassen, G. P. M. van Klink, M. Lutz, J. C. Chadwick, A. L. Spek, G. van Koten, *Dalton Trans.* **2011**, *40*, 8887; g) K. P. McGowan, K. A. Abboud, A. S. Veige, *Organometallics* **2011**, *30*, 4949.

[4] For representative symmetrical N donors NCN-pincer complexes, see: [N = amines]: a) O. A. Wallner, K. J. Szabó, *Org. Lett.* **2004**, *6*, 1829; b) J. Kjellgren; H. Sundén, K. J. Szabó, *J. Am. Chem. Soc.* **2004**, *126*, 474; H. Sundén, K. J. Szabó, *J. Am. Chem. Soc.* **2004**, *126*, 474; c) M. Q. Slagt, G. Rodrìguez, M. M. P. Grutters, R. J. M. K. Gebbink, W. Klopper, L. W. Jenneskens, M. Lutz, A. L. Spek, G. van Koten, *Chem. Eur. J.* **2004**, *10*, 1331; [N = imines]: d) K. Takenaka, M. Minakawa, Y. Uozumi, *J. Am. Chem. Soc.* **2005**, *127*, 12273; e) J. S. Fossey, M. L. Russell, K. M. A. Malik; C. J. Richards, *J. Organomet. Chem.* **2007**, *692*, 4843; C. J. Richards, *J. Organomet. Chem.* **2007**, *692*, 4843; [N = pyridines]: f) B. Soro, S. Stoccoro, G. Minghetti, A. Zucca, M. A. Cinellu, S. Gladiali, M. Manassero, M. Sansoni, *Organometallics* **2005**, *24*, 53; g) B. Soro, S. Stoccoro, G. Minghetti, A. Zucca, M. A. Cinellu, M. Manassero, S. Gladiali, *Inorg. Chim. Acta* **2006**, *359*, 1879; h) M. S. Yoon, R. Ramesh, J. Kim, D. Ryu, K. H. Ahn, *J. Organomet. Chem.* **2006**, *691*, 5927; [N = oxazolines]: i) H. Nishiyama, *Chem. Soc. Rev.* **2007**, *36*, 1133; j) Y. Motoyama, N. Makihara, Y. Mikami, K. Aoki; H. Nishiyama, *Chem. Lett.* **1997**, 951; H. Nishiyama, *Chem. Lett.* **1997**, 951; k) M. A. Stark; C. J. Richards, *Tetrahedron Lett.* **1997**, *38*, 5881; C. J. Richards, *Tetrahedron Lett.* **1997**, *38*, 5881; l) S. E. Denmark, R. A. Stavenger, A. M. Faucher, J. P. Edwards, *J. Org. Chem.* **1997**, *62*, 3375; m) M. A. Stark, G. Jones; C. J. Richards, *Organometallics* **2000**, *19*, 1282; C. J. Richards, *Organometallics* **2000**, *19*, 1282; n) T. Takemoto, S. Iwasa; H. Hamada, K. Shibatomi, M. Kameyama, Y. Motoyama; H. Nishiyama, *Tetrahedron Lett.* **2007**, *48*, 3397; H. Hamada, K. Shibatomi, M. Kameyama, Y. Motoyama; H. Nishiyama, *Tetrahedron Lett.* **2007**, *48*, 3397; o) A. Bugarin, B. T. Connell, *Organometallics* **2008**, *27*, 4357; p) T. Kimura, Y. Uozumi, *Organometallics* **2008**, *27*, 5159; [N = pyrazole]: q) C. M. Hartshorn, P. J. Steel, *Organometallics* **1998**, *17*, 3487; r) H. P. Dijkstra, M. D. Meijer, J. Patel, R. Kreiter, G. P. M. van Klink, M. Lutz, A. L. Spek, A. J. Canty, G. van Koten, *Organometallics* **2001**, *20*, 3159.

[5] a) X.-Q. Hao, Y.-N. Wang, J.-R. Liu, K-L. Wang, J.-F. Gong, M.-P. Song, *J. Organomet. Chem.* **2010**, *695*, 82.

[6] For a general review on unsymmetrical *ECE′* and *ECZ*-pincer Pd^{II} complexes, see: I. Moreno, R. SanMartin, B. Inés, M. T. Herrero, E. Domínguez, *Curr. Org. Chem.* **2009**, *13*, 878.

[7] For a related example of unsymmetrical NCN′-pincer complex incorporating an N-heterocyclic carbene functional group, see: N. Schneider, V. César, S. Bellemin-Laponnaz, L. H. Gade, *Organometallics* **2005**, *24*, 4886.

[8] G. Giambastiani, L. Luconi, R. L. Kuhlman, P. D. Hustad in *Olefin Upgrading Catalysis by Nitrogen-based Metal Complexes I* (Eds.: G. Giambastiani, J. Campora), Springer, London, **2011**, pp. 197–282, and references therein.

[9] L. Luconi, A. Rossin, G. Tuci, I. Tritto, L. Boggioni, J. J. Klosin; C. N. Theriault, G. Giambastiani, *Chem. Eur. J.* **2012**, *18*, 671; C. N. Theriault, G. Giambastiani, *Chem. Eur. J.* **2012**, *18*, 671.

[10] L. Luconi, A. Rossin, G. Tuci, S. Germain, E. Schulz, J. Hannedouche, G. Giambastiani; *ChemCatChem*, **2012**, DOI: 10.1002/cctc.201200389.

[11] L. Luconi, G. Giambastiani, A. Rossin; C. Bianchini, A. Lledós, *Inorg. Chem.* **2010**, *49*, 6811; C. Bianchini, A. Lledós, *Inorg. Chem.* **2010**, *49*, 6811.

[12] a) R. Mukherjee, *Coord. Chem. Rev.* **2000**, *203*, 151; b) S. Radia, A. Ramdania, Y. Lekchirib, M. Morcelletc, G. Crinic, J. Morcelletc, L. Janus, *Eur. Polym. J.* **2000**, *36*, 1885.

[13] An unique example of pirydylamido N,C,N′ dianionic systems in combination with Group IV metal complexes as polymerization pre-catalysts is mentioned in the following US patent application: G. R. Giesbrecht, T. M. Boller, A. Z. Voskoboynikov, A. F. Asachenko, M. V. Nikulin, A. A. Tsarev, US patent Applic, 2011/0098429 Al.

[14] For general reviews on the metal-mediated hydroamination reaction, see: a) K. D. Hesp, M. Stradiotto, *ChemCatChem* **2010**, *2*, 1192; b) G. Zi, *Dalton Trans.* **2009**, 9101; c) S. C. Chemler, *Org. Biomol. Chem.* **2009**, *7*, 3009; d) T. E. Müller, K. C. Hultzsch, M. Yus, F. Foubelo, M. Tada, *Chem. Rev.* **2008**, *108*, 3795; e) I. Aillaud, J. Collin, J. Hannedouche, E. Schulz, *Dalton Trans.* **2007**, 5105; f) R. Severin, S. Doye, *Chem. Soc. Rev.* **2007**, *36*, 1407; g) K. C. Hultzsch, *Adv. Synth. Catal.* **2005**, *347*, 367; h) K. C. Hultzsch, *Org. Biomol. Chem.* **2005**, *3*, 1819; i) S. Hong, T. J. Marks, *Acc. Chem. Res.* **2004**, *37*, 673; j) P. W. Roesky, T. E. Müller, *Angew. Chem.* **2003**, *115*, 2812; *Angew. Chem. Int. Ed.* **2003**, *42*, 2708; k) T. E. Müller, M. Beller, *Chem. Rev.* **1998**, *98*, 675.

[15] For a neutral Group IV metal-catalyzed hydroamination reaction of aminoalkenes, see: a) R. K. Thomson, J. A. Bexrud, L. L. Schafer, *Organometallics* **2006**, *25*, 4069; b) M. C. Wood, D. C. Leitch; C. S.

 © 2013 Wiley-VCH Verlag GmbH & Co. KGaA, Weinheim

These are not the final page numbers!

Yeung, J. A. Kozak, L. L. Schafer, *Angew. Chem.* **2006**, *119*, 358; C. S. Yeung, J. A. Kozak, L. L. Schafer, *Angew. Chem.* **2006**, *119*, 358; *Angew. Chem. Int. Ed.* **2006**, *46*, 354; c) S. Majumder, A. L. Odom, *Organometallics* **2008**, *27*, 1174; d) A. L. Gott, A. J. Clarke, G. J. Clarkson, P. Scott, *Chem. Commun.* **2008**, 1422; e) C. Müller, W. Saak, S. Doye, *Eur. J. Org. Chem.* **2008**, 2731; f) J. Cho, T. K. Hollis, T. R. Helgert, E. J. Valente, *Chem. Commun.* **2008**, 5001; g) D. C. Leitch, P. R. Payne; C. R. Dunbar, L. L. Schafer, *J. Am. Chem. Soc.* **2009**, *131*, 18246; C. R. Dunbar, L. L. Schafer, *J. Am. Chem. Soc.* **2009**, *131*, 18246; h) A. L. Reznichenko, K. C. Hultzsch, *Organometallics* **2010**, *29*, 24; i) J. A. Bexrud, L. L. Schafer, *Dalton Trans.* **2010**, *39*, 361; j) Y.-C. Hu; C.-F. Liang, J.-H. Tsai, G. P. A. Yap, Y.-T. Chang, T.-G. Ong, *Organometallics* **2010**, *29*, 3357; C.-F. Liang, J.-H. Tsai, G. P. A. Yap, Y.-T. Chang, T.-G. Ong, *Organometallics* **2010**, *29*, 3357; k) K. Manna, A. Ellern, A. D. Sadow, *Chem. Commun.* **2010**, *46*, 339; l) K. Manna, S. Xu, A. D. Sadow, *Angew. Chem.* **2011**, *123*, 1905–1908; *Angew. Chem. Int. Ed.* **2011**, *50*, 1865–1868; m) J. Cho, T. K. Hollis, E. J. Valente, J. M. Trate, *J. Organomet. Chem.* **2011**, *696*, 373; n) H. Kim, P. H. Lee, T. Livinghouse, *Chem. Commun.* **2005**, 5205; o) J. A. Bexrud, J. D. Beard, D. C. Leitch, L. L. Schafer, *Org. Lett.* **2005**, *7*, 1959; p) H. Kim, Y. K. Kim, J. H. Shim, M. Kim, M. Han, T. Livinghouse, P. H. Lee, *Adv. Synth. Catal.* **2006**, *348*, 2609; q) D. A. Watson, M. Chiu, R. G. Bergman, *Organometallics* **2006**, *25*, 4731; r) A. L. Gott, A. J. Clarke, G. J. Clarkson, P. Scott, *Organometallics* **2007**, *26*, 1729; s) L. Xiang, H. Song, G. Zi, *Eur. J. Inorg. Chem.* **2008**, 1135; t) G. Zi, Q. Wang, L. Xiang; H. Song, *Dalton Trans.* **2008**, 5930; H. Song, *Dalton Trans.* **2008**, 5930; u) G. Zi, X. Liu, L. Xiang; H. Song, *Organometallics* **2009**, *28*, 1127; H. Song, *Organometallics* **2009**, *28*, 1127; v) G. Zi, F. Zhang, L. Xue, L. Ai; H. Song, *J. Organomet. Chem.* **2010**, *695*, 730; H. Song, *J. Organomet. Chem.* **2010**, *695*, 730; w) G. Zi, F. Zhang, L. Xiang, Y. Chen, W. Fang; H. Song, *Dalton Trans.* **2010**, *39*, 4048; H. Song, *Dalton Trans.* **2010**, *39*, 4048; x) A. Mukherjee, S. Nembenna, T. K. Sen, S. Pillai Sarish, P. Kr. Ghorai; H. Ott, D. Stalke, S. K. Mandal; H. W. Roesky, *Angew. Chem.* **2011**, *123*, 4054; H. Ott, D. Stalke, S. K. Mandal; H. W. Roesky, *Angew. Chem.* **2011**, *123*, 4054; *Angew. Chem. Int. Ed.* **2011**, *50*, 3968; y) T. R. Helgert, T. K. Hollis, E. J. Valente, *Organometallics* **2012**, *31*, 3002.

[16] a) C. Bianchini, G. Giambastiani, G. Mantovani, A. Meli, D. Mimeau, *J. Organomet. Chem.* **2004**, *689*, 1356; b) P. Barbaro; C. Bianchini, G. Giambastiani, I. Guerrero Rios, A. Meli, W. Oberhauser, A. M. Segarra, L. Sorace, A. Toti, *Organometallics* **2007**, *26*, 4639; C. Bianchini, G. Giambastiani, I. Guerrero Rios, A. Meli, W. Oberhauser, A. M. Segarra, L. Sorace, A. Toti, *Organometallics* **2007**, *26*, 4639; c) C. Bianchini, G. Giambastiani, I. Guerrero Rios, A. Meli, W. Oberhauser, L. Sorace, A. Toti, *Organometallics* **2007**, *26*, 5066.

[17] M. M. Salter, J. Kobayashi, Y. Shimizu, S. Kobayashi, *Org. Lett.* **2006**, *8*, 3533.

[18] Y.-J. Wu; H. He, A. L'Heureux, *Tetrahedron Lett.* **2003**, *44*, 4217; H. He, A. L'Heureux, *Tetrahedron Lett.* **2003**, *44*, 4217.

[19] Other "ligand-free" and/or microwave-free Cu-mediated conditions applied to this specific Ullmann coupling gave (in our hands) decreased yields of 25–35%; see also a) A. Correa; C. Bolm, *Adv. Synth. Catal.* **2007**, *349*, 2673; C. Bolm, *Adv. Synth. Catal.* **2007**, *349*, 2673; b) H.-J. Cristau, P. P. Cellier, J.-F. Spindler, M. Taillefer, *Eur. J. Org. Chem.* **2004**, 695.

[20] G. Menozzi, L. Mosti, P. Schenone, *J. Heterocycl. Chem.* **1987**, *24*, 1669.

[21] C. S. Cho, D. K. Lim, N. H. Heo, T.-J. Kim, S. C. Shim, *Chem. Commun.* **2004**, 104.

[22] M. G. Kelly, J. Kincaid, M. Duncton, K. Sahasrabudhe, S. Janagani, R. B. Upasani, G. Wu, Y. Fang, Wei, Z.-L. US patent 2006/0194801 Al, pag 39.

[23] J. A. Joule, K. Mills, *Heterocyclic Chemistry, 5th ed.*, Wiley, Chichester, **2010**, pp. 718.

[24] This coexistence is reasonably caused by the combination of three factors: <1) disorder present on the dimethylamido ligands, 2) the (very) low-temperature data collection, and 3) the employment of 2D CCD X-ray detectors.

[25] In a similar manner to **13** and **14**, two almost identical molecules are present in the asymmetric unit, which are related to each other through a C_2 pseudosymmetry axis along the *b* direction; consequently, the same chemical species is "seen" as two structurally different molecules; see also ref. [9]; half of a pentane molecule was found as part of the asymmetric unit of **18** as a solvent molecule of crystallization.

[26] The calculated index of trigonality for each structure is 0.16, 0.22, 0.21, and 0.22 for **17**–**20**, respectively; see also A. W. Addison, T. N. Rao, J. Reedijk, J. van Rijn, G. C. Verschoor, *J. Chem. Soc. Dalton Trans.* **1984**, 1349.

[27] For related structures containing M–amido bonds, see also: [Zr]: a) see refs [10,15u]; b) T. K. Panda; H. Tsurugi, K. Pal; H. Kaneko, K. Mashima, *Organometallics* **2010**, *29*, 34; H. Tsurugi, K. Pal; H. Kaneko, K. Mashima, *Organometallics* **2010**, *29*, 34; c) see also ref. [3d]; [Hf]: d) K. Nienkemper, G. Kehr, S. Kehr, R. Frohlich, G. Erker, *J. Organomet. Chem.* **2008**, *693*, 1572; e) see also refs [3d,10,27b].

[28] For related structures containing M–$N_{pyrazolyl}$ bonds, see also: [Zr]: a) A. Otero, J. Fernandez-Baeza, J. Tejeda, A. Lara-Sanchez, S. Franco, J. Martinez-Ferrer, M. P. Carrion, I. Lopez-Solera, A. M. Rodriguez, L. F. Sanchez-Barba, *Inorg. Chem.* **2011**, *50*, 1826; [Hf]: b) A. Otero, J. Fernandez-Baeza, A. Antinolo, J. Tejeda, A. Lara-Sanchez, L. Sanchez-Barba, M. Fernandez-Lopez, I. Lopez-Solera, *Inorg. Chem.* **2004**, *43*, 1350.

[29] For related structures containing M–Ar bonds, see also: [Zr]: a) M. Bouwkamp, D. van Leusen, A. Meetsma, B. Hessen, *Organometallics* **1998**, *17*, 3645; b) R. J. Rubio, G. T. S. Andavan, E. B. Bauer, T. K. Hollis, J. Cho, F. S. Tham, B. Donnadieu, *J. Organomet. Chem.* **2005**, *690*, 5353; [Hf]: c) see also ref. [3c]; d) H. Tsurugi, K. Yamamoto, K. Mashima, *J. Am. Chem. Soc.* **2011**, *133*, 732.

[30] The theoretical Mulliken electronic charge on the pyrazolyl moieties of **13** and **15** did not show any relevant difference in the nucleophilic character of the pyridinic nitrogen atom on both systems; N_{py} = 0.344 and 0.323 e for **13** and **15**.

[31] For a selected example of cationic Zr complexes that operate under mild reaction conditions, see: X. Wang, Z. Chen, X.-L. Sun, Y. Tang, Z. Xie, *Org. Lett.* **2011**, *13*, 4758.

[32] For rare examples of neutral Group IV complexes that catalyze the hydroamination of secondary aminoalkenes, see refs [15h, m, x, 31].

[33] C. Müller, R. Koch, S. Doye, *Chem. Eur. J.* **2008**, *14*, 10430.

[34] Calculated relative internal energies *E* have been reported for both systems; however, the relative Gibbs energy values *G* are not provided because they are not relevant to the conclusions herein and are beyond the scope of the present work.

[35] Although the authors are aware of the relatively high energy values calculated for TS4 (with both substrates) for reactions at room temperature, the present study is aimed at addressing, at the molecular level, the existence of cooperative and favorable interactions between substrate(s) and complex; the supposed operative mechanism is assumed on the basis of several reported precedents (see also refs. [15, 33]), and it fits well with all the other experimental outcomes; accordingly, a very similar behavior has been computationally ascertained for both substrates, along the most classical pathway assumed for this chemistry; apart from this finding, the authors are convinced that an in-depth theoretical study is needed to clarify computationally the truly operative mechanistic path.

[36] Slightly decreased conversions of **I** measured throughout the kinetic tests (relative to the values reported in Table 4) are likely due to diffusive limiting factors for runs accomplished in a J-Young NMR tube (see the Experimental Section).

[37] To the best of our knowledge, C,C,C-N-heterocyclic carbene pincer complexes based on Group IV transition metals represent the only pincer-type systems to date to be active catalysts in the hydroamination reaction of unactivated alkenes; all these complexes typically require extremely severe reaction conditions to promote the cycliza-

 © 2013 Wiley-VCH Verlag GmbH & Co. KGaA, Weinheim

tion of variably substituted primary aminoalkenes; see refs. [15f, m, z].
[38] O. S. Zhukova, L. P. Lazareva, A. P. Artem′yanov, *Russ. J. Electrochem.* **2001**, *37*, 629.
[39] CrysAlisCCD 1.171.31.2 (release 07–07–2006); CrysAlis171.NET, Oxford Diffraction Ltd.
[40] CrysAlis RED 1.171.31.2 (release 07–07–2006); CrysAlis171.NET, Oxford Diffraction Ltd.
[41] A. Altomare, M. C. Burla, M. Camalli, G. L. Cascarano; C. Giacovazzo, A. Guagliardi, A. G. Moliterni, G. Polidori, R. Spagna, *J. Appl. Crystallogr.* **1999**, *32*, 115–119; C. Giacovazzo, A. Guagliardi, A. G. Moliterni, G. Polidori, R. Spagna, *J. Appl. Crystallogr.* **1999**, *32*, 115–119.
[42] G. M. Sheldrick, SHELXL, Göttingen, **1997**.
[43] L. J. Farrugia, *J. Appl. Crystallogr.* **1997**, *30*, 565.
[44] Gaussian 09, Revision A.02, M. J. Frisch, G. W. Trucks, H. B. Schlegel, G. E. Scuseria, M. A. Robb, J. R. Cheeseman, G. Scalmani, V. Barone, B. Mennucci, G. A. Petersson, H. Nakatsuji, M. Caricato, X. Li, H. P. Hratchian, A. F. Izmaylov, J. Bloino, G. Zheng, J. L. Sonnenberg, M. Hada, M. Ehara, K. Toyota, R. Fukuda, J. Hasegawa, M. Ishida, T. Nakajima, Y. Honda, O. Kitao, H. Nakai, T. Vreven, J. A. Montgomery, Jr., J. E. Peralta, F. Ogliaro, M. Bearpark, J. J. Heyd, E. Brothers, K. N. Kudin, V. N. Staroverov, R. Kobayashi, J. Normand, K. Raghavachari, A. Rendell, J. C. Burant, S. S. Iyengar, J. Tomasi, M. Cossi, N. Rega, J. M. Millam, M. Klene, J. E. Knox, J. B. Cross, V. Bakken, C. Adamo, J. Jaramillo, R. Gomperts, R. E. Stratmann, O. Yazyev, A. J. Austin, R. Cammi, C. Pomelli, J. W. Ochterski, R. L. Martin, K. Morokuma, V. G. Zakrzewski, G. A. Voth, P. Salvador, J. J. Dannenberg, S. Dapprich, A. D. Daniels, Ö. Farkas, J. B. Foresman, J. V. Ortiz, J. Cioslowski, D. J. Fox, Gaussian, Inc. Wallingford CT, **2009**..
[45] Y. Zhao, D. G. Truhlar, *Theor. Chem. Acc.* **2008**, *120*, 215–241.
[46] a) P. J. Hay, W. R. Wadt, *J. Chem. Phys.* **1985**, *82*, 270–283; b) W. R. Wadt, P. J. Hay, *J. Chem. Phys.* **1985**, *82*, 284–298.
[47] a) A. Höllwarth, M. Böhme, S. Dapprich, A. W. Ehlers, A. Gobbi, V. Jonas, K. F. Köhler, R. Stegmann, A. Veldkamp, G. Frenking, *Chem. Phys. Lett.* **1993**, *208*, 237–240; b) A. W. Ehlers, M. Böhme, S. Dapprich, A. Gobbi, A. Höllwarth, V. Jonas, K. F. Köhler, R. Stegmann, A. Veldkamp, G. Frenking, *Chem. Phys. Lett.* **1993**, *208*, 111–114.
[48] The CP2K developers group. http://www.cp2k.org.
[49] S. Goedecker, M. Teter, J. Hutter, *J. Phys. Rev. B* **1996**, *54*, 1703.
[50] J. P. Perdew, K. Burke, M. Ernzerhof, *Phys. Rev. Lett.* **1997**, *78*, 1396(E).
[51] S. J. Grimme, J. Antony, S. Ehrlich; H. Krieg, *Comput. Chem.* **2010**, *132*, 154104.
[52] CCDC-897882 (**13**), CCDC-897880 (**14**), CCDC-897878 (**17**), CCDC-897881 (**18** $1/2C_5H_{12}$), CCDC-897879 (**19**), and CCDC-897883 (**20**) contain the supplementary crystallographic data for this paper. These data can be obtained free of charge from The Cambridge Crystallographic Data Centre via www.ccdc.cam.ac.uk/data_request/cif.

Received: October 11, 2012
Published online: ■■ ▮▮, 0000

 © 2013 Wiley-VCH Verlag GmbH & Co. KGaA, Weinheim

These are not the final page numbers!

Changing the order of the "factors" can (somehow) change the result! Neutral Zr^{IV} and Hf^{IV} diamido complexes stabilized by unsymmetrical dianionic N,C,N′-pincer ligands have been prepared (see picture) and successfully employed as good catalyst candidates for the efficient and mild intramolecular hydroamination/cyclization of primary aminoalkenes.

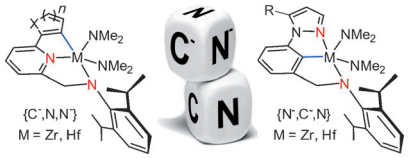

Organometallic Catalysis

© 2013 Wiley-VCH Verlag GmbH & Co. KGaA, Weinheim